The Abdus Salam
International Centre for Theoretical Physics

United Nations
Educational, Scientific
and Cultural Organization

International Atomic
Energy Agency

SMR: 1643/9

WINTER COLLEGE ON OPTICS ON OPTICS AND PHOTONICS IN NANOSCIENCE AND NANOTECHNOLOGY

(7 - 18 February 2005)

"Electrons and Excitons in Semiconductor Nanostructures

presented by:

K. Rustagi
Indian Institute of Technology
Mumbai
India

Electrons And Excitons in Semiconductor Nanostructures

Kailash Rustagi

IIT,Mumbai ,India

rustagi@ phy.iitb.ac.in

Till 31 October 2004 at:

Centre for Advanced Technology, Indore

PROBLEM:
NANOSTRUCTURES ARE MESOSCOPIC:

***i.e.*, MUCH LARGER THAN SMALL MOLECULES**

MUCH TOO SMALL TO BE TREATED AS INFINITE SOLID;

K_x, $K_{y,}$ K_z NOT A GOOD QUANTUM NUMBER (DIMENSIONALITY IMPORTANT)

LARGE FRACTION OF ATOMS AT THE SURFACE (RECONSTRUCTION)

SOLUTION TWO APPROACHES

BOTTOM UP i.e. MOLECULAR METHODS AT LARGER SIZES

TOP DOWN i.e. SOLID STATE METHODS i.e. BULK SOLID

WITH QUANTUM CONFINEMENT EFFECTS

THIS IS ELABORATED IN THESE LECTURES

GOOD APPROXIMATION IF STRUCTURE IS STABILIZED TO BULK LIKE
..... MOSTLY TRUE FOR SEMICONDUCTORS

BUT SOME OTHER QUANTUM CONFINED SYSTEMS TOO

$$\Delta x \Delta p \geq \hbar/2$$

$$KE = < p^2/2m >$$

$$\geq < p^2/2m > - < p >^2/2m$$

$$\geq (\Delta p)^2/2m$$

$$\geq \hbar^2/(8m(\Delta x)^2)$$

Discreteness $\Delta E >\sim kT$ has thermodynamic implications,

also influences electromagnetic response and relaxation pathways

SPECTROSCOPY IS IMPORTANT

Evolution of solutions (Top down)

Effective mass approximation (EMA)

-single band

-multiband

EMPIRICAL TIGHT BINDING METHOD

Pseudo-potential Method

COMPLICATION: SHAPES

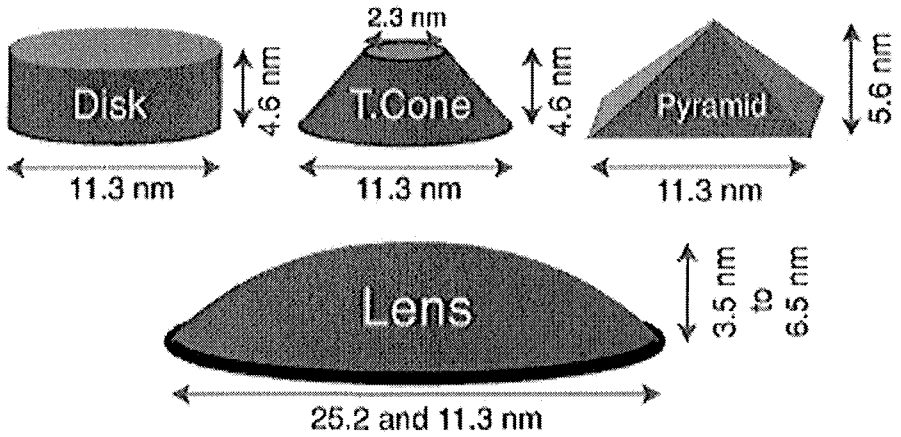

FIG. 1. Shapes and sizes of InAs/GaAs dots considered. Disk, truncated cone (T.Cone), pyramid, and lens.

Gabriel Bester and Alex Zunger
PHYSICAL REVIEW B 71, 045318 (2005)

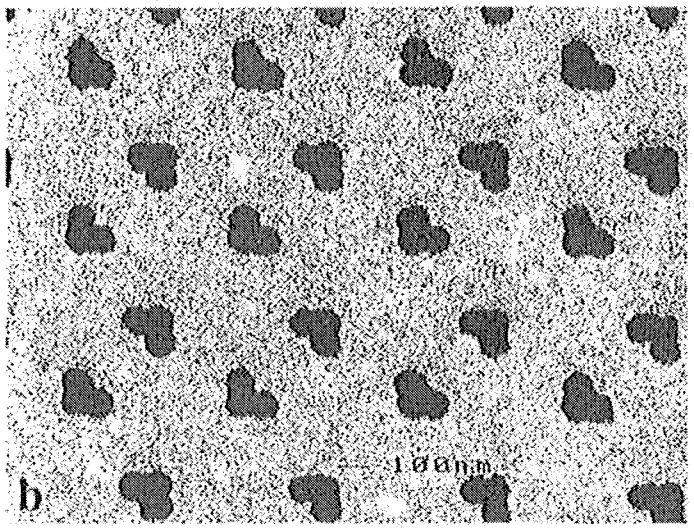

B.Lamprecht *etal*
Appl Phys.B68,419(1999)

QUANTUM CONFINEMENT IN π ELECTRON SYSTEMS

H. Kuhn Fortsch Chem Org Nat 16,169(1958), 17,404 (1959)

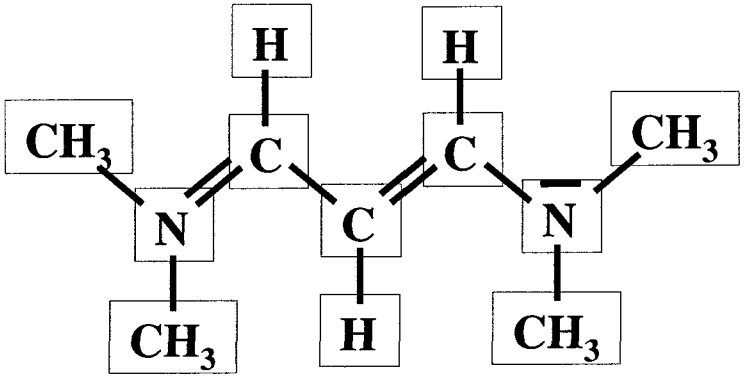

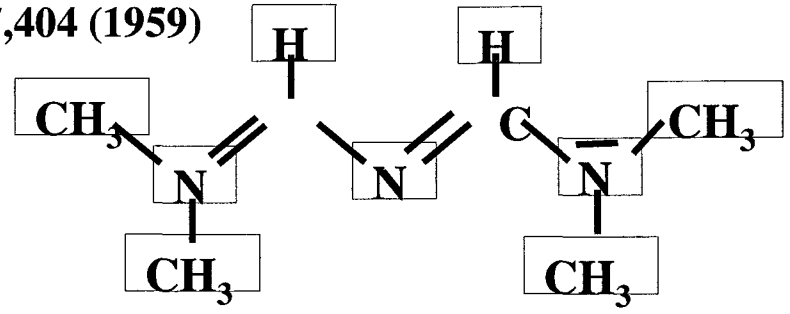

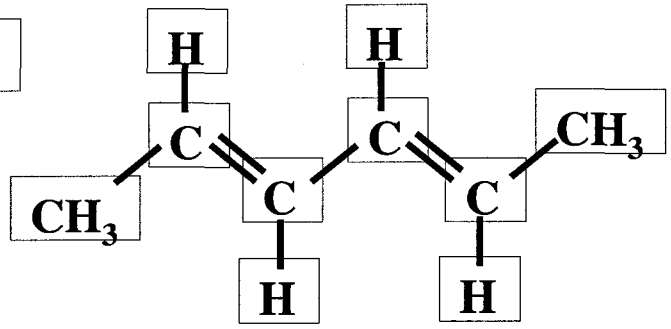

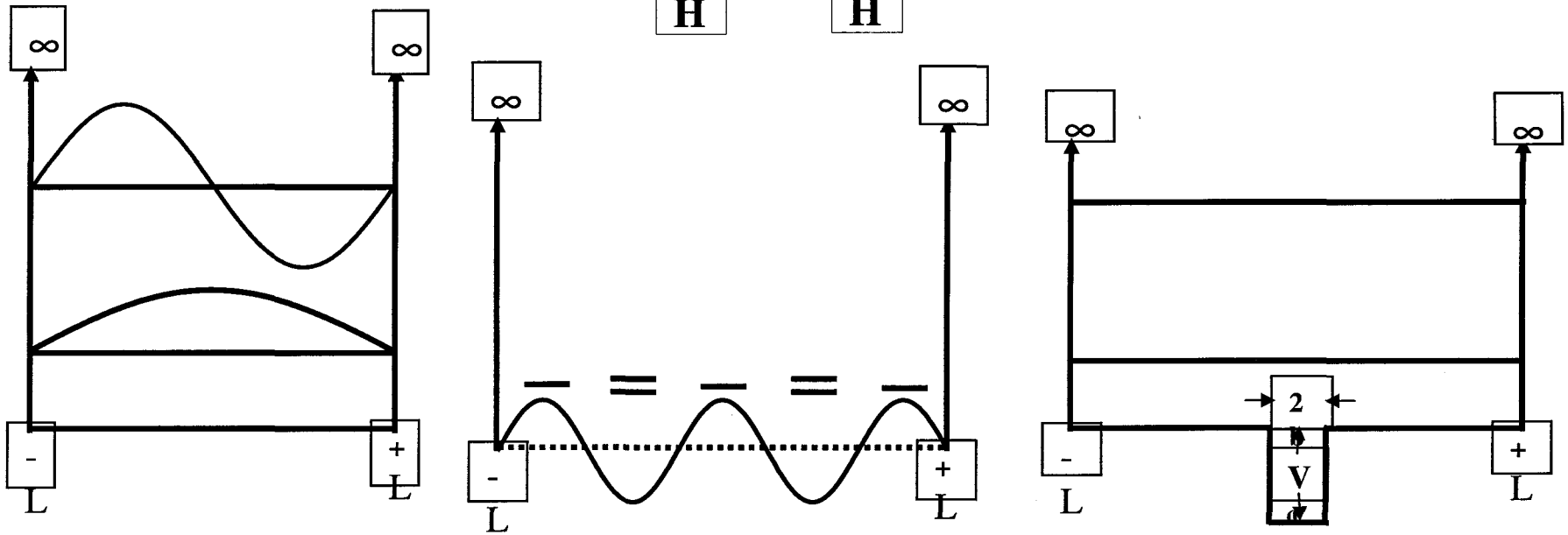

NONLINEAR SUSCEPTIBILITIES(Rustagi,Ducuing,Mehendale(1974,79))

$$\alpha = \frac{4L^4}{a_0} \sum_{n=1}^{N} \{ \frac{-2}{3\pi^2 n^2} + \frac{10}{3\pi^4 n^4} \}$$

$$\gamma = \frac{128\ L^{10}}{a_0{}^3 e^2} \sum_{n=1}^{N} \{ \frac{-2}{9\pi^6 n^6} + \frac{140}{3\pi^8 n^8} - \frac{440}{\pi^{10} n^{10}} \}$$

$$\cong \frac{256\ L^5 d^5}{45\, a_0{}^3 e^2 \pi^6}$$

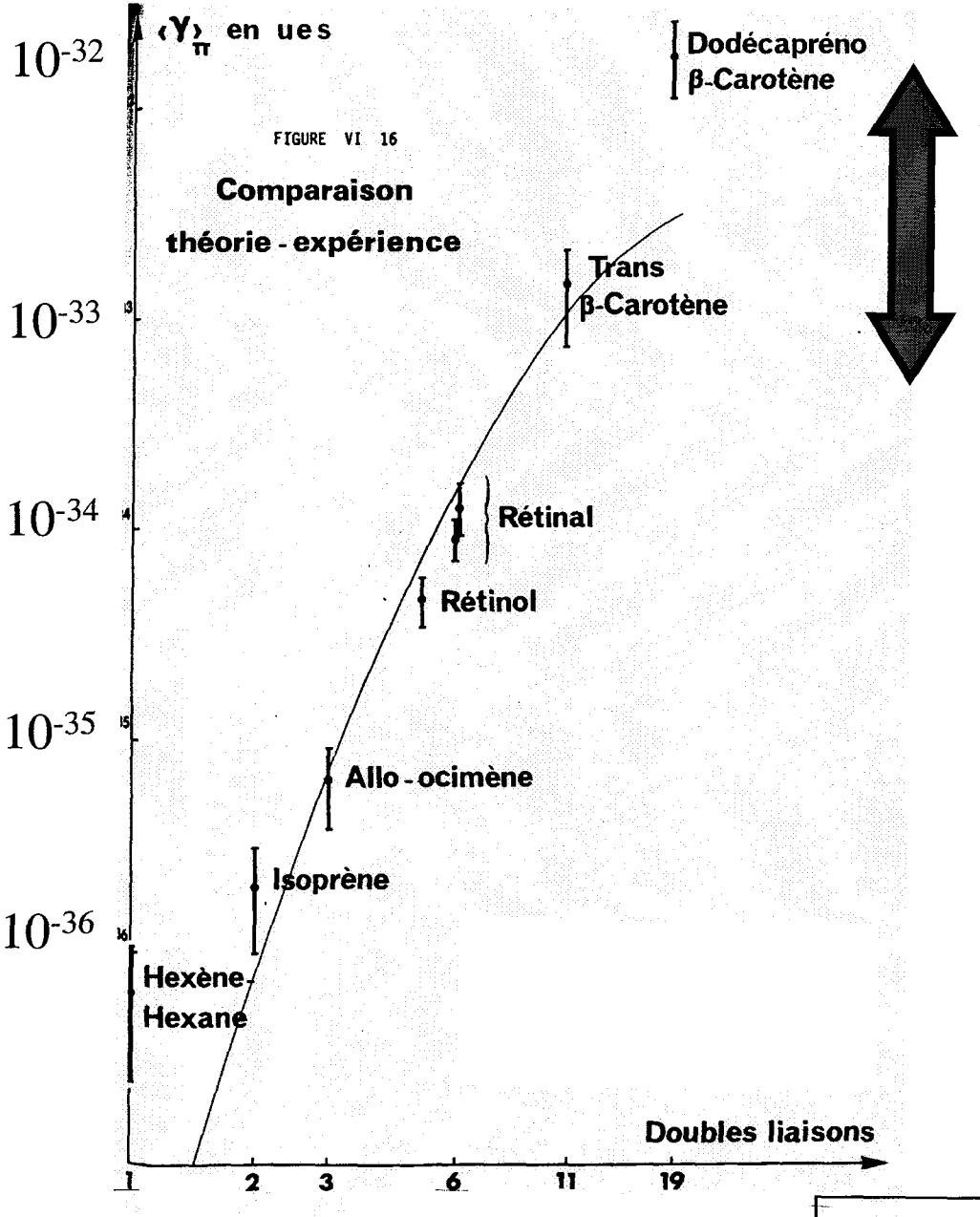

FIGURE VI 16

Comparaison

théorie - expérience

RESONANT ENHANCEMENT

J.-P.Hermann These(1974)

$$H_0 = p^2/2m + \frac{1}{2} m\omega_0^2 x^2$$

$$H = p^2/2m + \frac{1}{2} m\omega_0^2 x^2 - \frac{eEx}{m\omega_0^2}$$

$$H = p^2/2m + \frac{1}{2} m\omega_0^2 (x - \frac{eE}{m\omega_0^2})^2 - (\frac{eE}{m\omega_0^2})^2$$

$$\alpha = \frac{e^2}{m\omega_0^2}$$

$$\beta = \gamma = 0$$

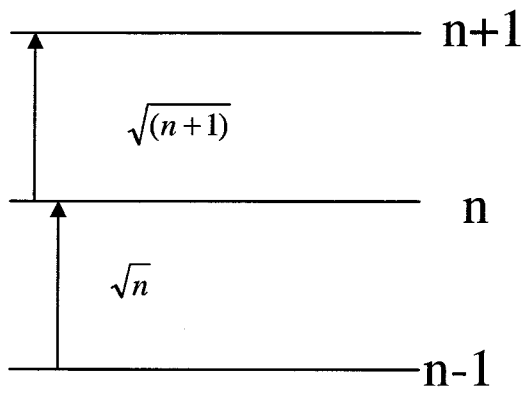

One dimensional metal

$$\lambda_{\max} \sim L$$

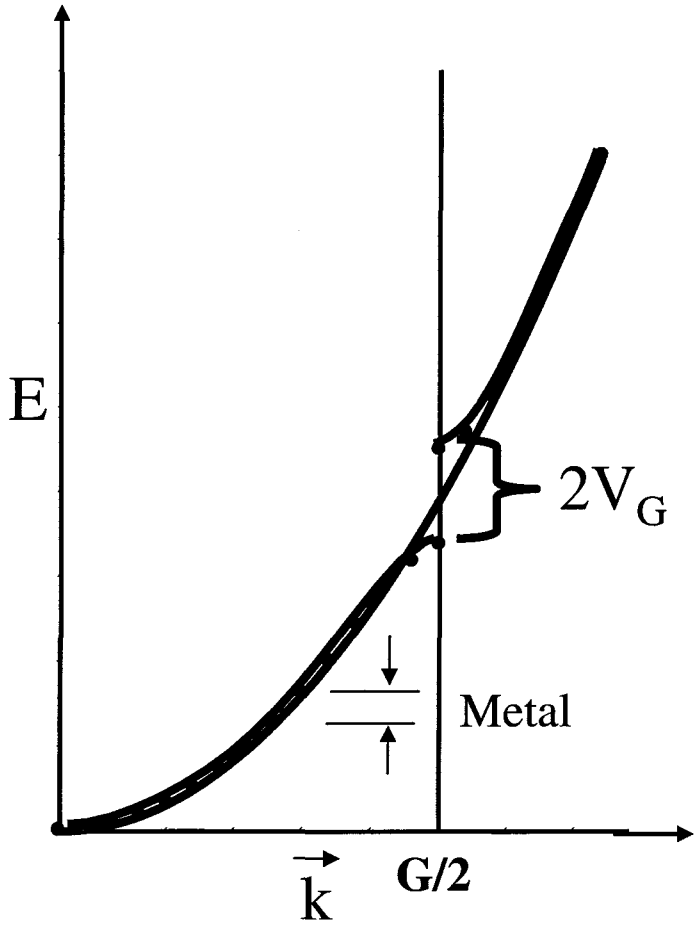

One dimensional semiconductor

$$\lambda_{\max} \sim \lambda_{gap} + A / L^2$$

Localized perturbation in the middle lowers energy of alternate levels

$$\lambda_{\max} \sim AL \pm B / L$$

ENVELOPE APPROXIMATION GOOD

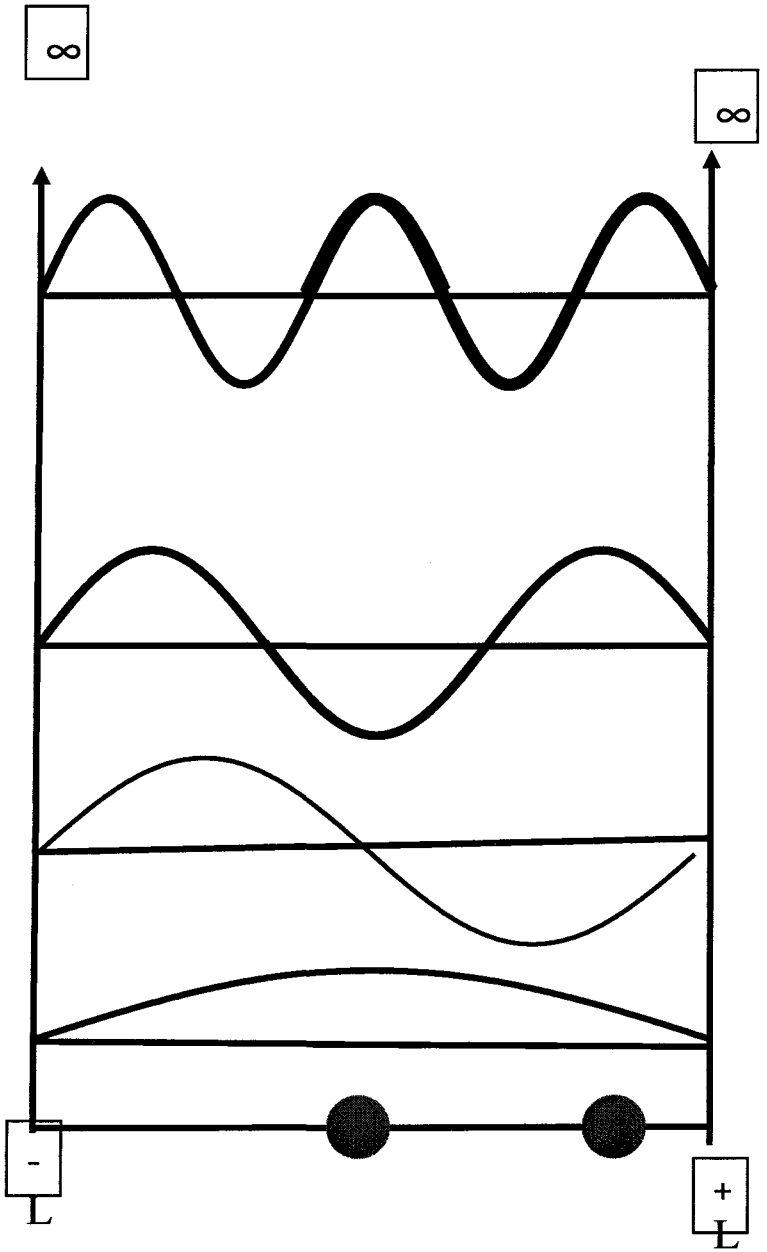

$$E_n^{(1)} = < n \mid H' \mid n >$$

....depends on $|\psi|^2$

at impurity position

IN QUANTUM CONFINED SYSTEMS EFFECT OF SUBSTITUTION DEPENDS ON POSITION OF THE IMPURITY

For linear conjugated chains:

Rustagi and Ducuing Opt Comm 10,258(1974)

Nonlinearity increases rapidly with chain length

And with "anharmonicity"

which can be increased by chemical substitution

Mehendale and Rustagi Opt Comm 28,359(1979)

In NONLINEAR OPTICAL PROPERTIES OF POLYMERS (MRS, 1988)
S.H. Stevenson et al (DUPONT)

.... as predicted by Rustagi, significant enhancement of third-order nonlinear polarizability in a linear conjugated system can be achieved by simple structural modifications which act mainly to increase the anharmonicity of its representative effective oscillator.

For fullerenes: depolarization field reduces the effective field substantially

Implying much smaller nonlinearity than for linear molecules

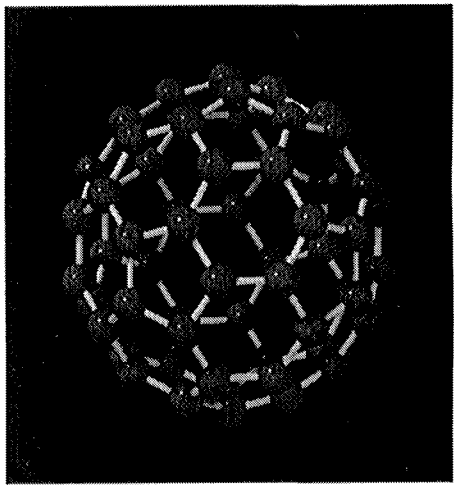

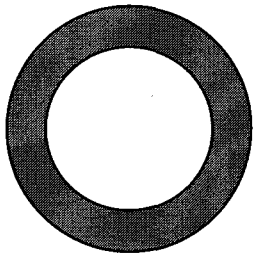

ICOSAHEDERAL PSEUDOPOTENTIAL

Nair
1992

Dimensionality matters a lot for nonlinear response!

Intrinsic Bulk Semiconductor

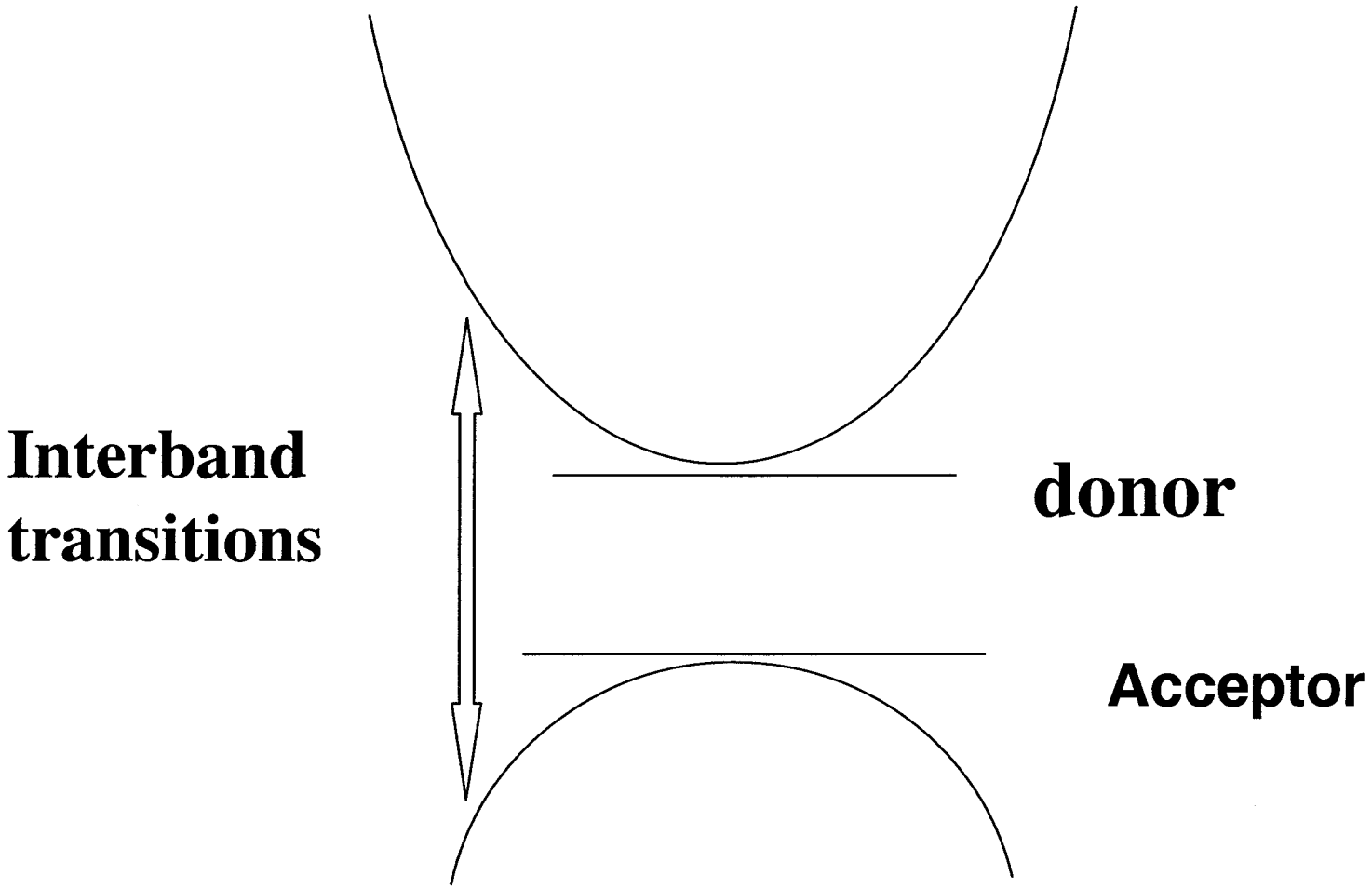

EFFECTIVE MASS OR ENVELOPE FUNCTION METHOD

$$H = KE + V_{periodic} + V_{imp}$$

$$\Psi(r) = \psi(r) u_c(r)$$

$$(p^2 / 2m_{ij}^{*} + V_{imp})\psi(\vec{r}) = \varepsilon\psi(\vec{r})$$

m_{ij}^{*} **effective mass**

$$\hbar^2 / m_{ij}^{*} = \partial^2 E / \partial k_i \partial k_j$$

Main Assumption : V_{imp} varies slowly over lattice constant

GENERALIZED TO DEGENERATE VALENCE BANDS

Kohn and Luttinger (1955)
for shallow impurities

R J Elliot (1956) for excitons

Quantum confined systems

$$V_{imp} \longrightarrow V_{confinement}$$

$$V_{confinement} = V(z) \qquad \textbf{Quantum Well}$$

$$V_{confinement} = V(x, y) \qquad \textbf{Quantum Wire}$$

$$V_{confinement} = V(x, y, z) \qquad \textbf{Quantum Dot/BOX}$$

$$\Psi(r) = \psi(r) u_c(r)$$

$$(p^2 / 2m_{ij}^{*} + V_{confinement})\psi(\vec{r}) = \varepsilon\psi(\vec{r})$$

Quantum Wells

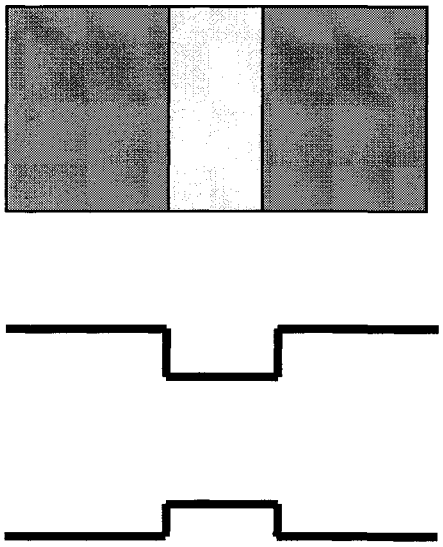

Assume: confinement potential slowly varying

u_c, u_v same in the two materials

SOLVE ENVELOPE FUNCTION EQUATIONS

MATCH AT THE BOUNDARY z= +L,-L

PROBLEMS:

1. Barrier height? Quite often inferred indirectly from optical spectroscopy using rather simple theories, so still changing

2. $m^*_{barrier} \neq m^*_{well}$

$$p_z^2/2m^* \rightarrow p_z(1/m^*(z))p_z$$

e.g., M.Altarelli in *Interfaces,Quantum wells,and superlattices*,

eds Leavens and Taylor,Plenum (1988)

Refs: G.Bastard" Wave mechanics applied to semiconductor heterostructures,Les Edision de Phys(1988)

C.Weisbuch and B.Vinter Quantum Semiconductor structures,Academic (1991)

Spherical Quantum Dot

$$\psi_{nlm}(r,\theta,\phi) = \frac{2^{1/2}}{R^{3/2}} \frac{1}{j_{l+1}(\varsigma_{nl})} j_l\left(\varsigma_{nl}\frac{r}{R}\right) Y_{lm}(\theta,\phi),$$

$$E_0 = \frac{\hbar^2}{2m^* R^2}\varsigma_{nl}^2$$

ς_{nl} zeros of the spherical Bessel function.

Cylindrical Quantum Dot

$$\Psi_{\nu,n,s} = \frac{\sqrt{2}}{\sqrt{z_0}} \sin\left(\frac{\nu\pi}{z_0}(z+z_0/2)\right) \psi_{ns}(\rho,\phi), \qquad \nu = 1,2,3,.$$

$$\psi_{ns}(\rho,\phi) = \frac{2}{\rho_0} \frac{1}{\sqrt{\pi} J_{n+1}(\alpha_{ns})} J_n\left(\alpha_{ns}\frac{\rho}{\rho_0}\right) \zeta_n(\phi)$$

$$n = 1,2,\ldots, \qquad s = 1,2,\ldots,$$

MULTI BAND EFFECTIVE MASS CALCULATION

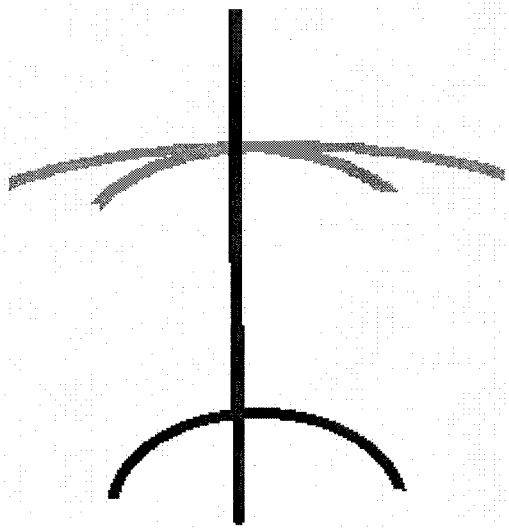

Γ_8

Γ_7

$$u_{-3/2} = |X - iY> \downarrow / \sqrt{2}$$

$$u_{3/2} = -|X + iY> \uparrow / \sqrt{2}$$

$$u_{1/2} = -|X + iY> \downarrow / \sqrt{6} + \sqrt{2/3}|Z> \uparrow$$

$$u_{1/2} = |X - iY> \uparrow / \sqrt{6} + \sqrt{2/3}|Z> \downarrow$$

$$E(k) = (\hbar^2 / 2m)(\gamma_1 k^2$$

$$\pm[4\gamma_2^2 \ k^4 + 12(\gamma_3^2 - \gamma_2^2)(k_x^2 k_y^2 + k_y^2 k_z^2 + k_x^2 k_z^2)]^{1/2})$$

J.M.Luttinger Phys Rev 102,1030(1956)

$$H = (\hbar^2/2m)\begin{pmatrix} P_{3/2} & -S & R & 0 \\ -S^* & P_{1/2} & 0 & R \\ R^* & 0 & P_{-1/2} & S \\ 0 & R^* & S^* & P_{-3/2} \end{pmatrix}$$

$$P_{3/2} = P_{-3/2} = \gamma_1 k^2 + \gamma_2 (k_x^2 + k_y^2 - 2k_z^2)$$

$$P_{1/2} = P_{-1/2} = \gamma_1 k^2 - \gamma_2 (k_x^2 + k_y^2 - 2k_z^2)$$

$$R = -(\sqrt{3}/2)(\gamma_2 + \gamma_3)(k_x - ik_y)^2 + \sqrt{3}/2(\gamma_3 - \gamma_2)(k_x + ik_y)^2$$

$$S = 2/\sqrt{3}\gamma_3 k_z (k_x - ik_y)$$

γ_i **Luttinger parameters**

$$\vec{k} = -i\vec{\nabla}$$

To get envelope equation

J.M.Luttinger Phys Rev 102,1030(1956)

For semiconductor quantum dots grown by soft chemical methods confinement potential is relatively large and can be assumed to be infinite.
In semiconductors confined by a larger gap semiconductor the band offset is generally small ~ 0.1 to 1eV Resulting finite well problem is generally more difficult to solve

Also boundary conditions uncertain, but perturbative treatment possible for small variations in shape.

Empirical Tight Binding method
P.E. Lippens and M. Lannoo, sps*
Phys. Rev. B 39, 10 935 (1989)

S. Sapra, N. Shanthi, and D.D. Sarma,
Phys. Rev. B 66, 205202 (2002)
S. Sapra, and D.D. Sarma,
Phys. Rev. B 69, 125304 (2004)
for II-VI COMPOUND QUANTUM DOTS sp^3d^5

"Direct diagonalization methods are practical only for cluster sizes containing less than ;1500 atoms. For larger clusters, we use the Lanczos iterative method"

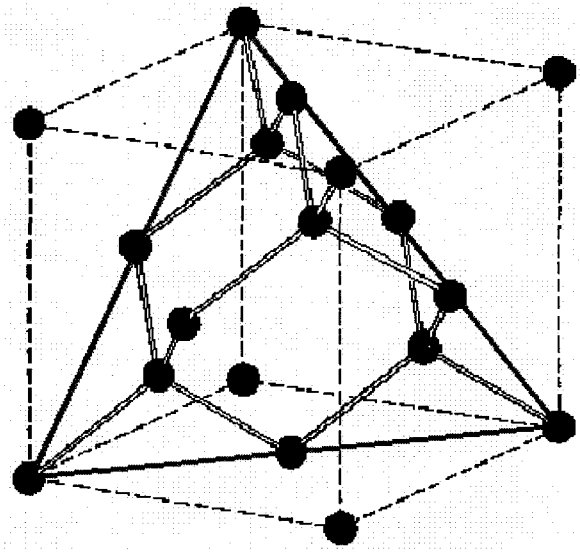

			ZnS	ZnSe	ZnTe	CdS	CdSe	CdTe
a(Å)			5.41	5.67	6.10	5.82	6.05	6.48
Ns	*N*	*d*(Å)						
12	1285		36.49	38.24	41.14	39.25	40.80	43.70

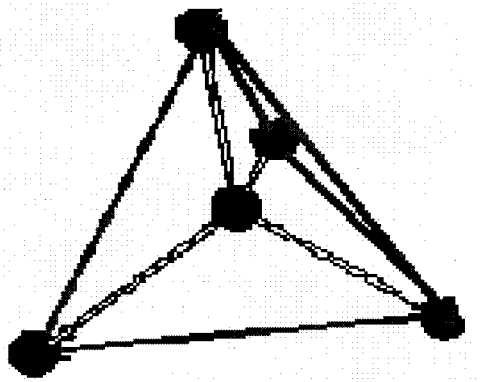

EFFECTIVE BOND ORBITAL MODEL(Y.C. CHANG)

REDUCED NUMBER OF ORBITALS CAN MANAGE LARGER PARTICLES

ALSO FEWER PARAMETERS, BUT NOT FROM BASIC THEORIES

VALENCE BAND MODEL

Y.-C. Chang PRB 37,8215(1988)

$$6orbitals = x\uparrow, x\downarrow, y\uparrow, y\downarrow, z\uparrow, z\downarrow,$$

$$< R\alpha \mid H \mid R'\alpha' >= E_p \delta_{R,R'} \delta_{\alpha\alpha'} +$$

$$\sum_{\tau} \delta_{R-R',\tau} \{ E_{xy} \tau_\alpha \tau_{\alpha'} (1-\delta_{\alpha\alpha'}) + [E_{xx} \tau_\alpha^2 + E_{zz}(1-\tau_\alpha^2)] \delta_{\alpha\alpha'} \}$$

$|\boldsymbol{R},\alpha>$ orbital at $\boldsymbol{R}$ and α= x,y,z τ nearest neighbor displacement vectors

E_p *site energy,* Exx, Exy, Ezz *interaction energies*

Conduction Valence Band Model

$$\langle \mathbf{R}s \mid H \mid \mathbf{R}'s \rangle = E_s \delta_{\mathbf{R},\mathbf{R}'} + \sum_{\tau} E_{ss} \delta_{\mathbf{R}-\mathbf{R}',\tau}$$

$$\langle \mathbf{R}s \mid H \mid \mathbf{R}'\alpha \rangle = \sum_{\tau} E_{sx} \tau_\alpha \delta_{\mathbf{R}-\mathbf{R}',\tau} .$$

Nair,Ramaniah,Rustagi PRB 45,5969(1992)

To include spin orbit coupling

Form combinations transforming like j=3/2,or j=1/2 states

Shift j=3/2 like states above j=1/2 like states

The new matrix elements are related to the old ones by C(α,σ; J,M) Clebsch-Gordon coefficients

$$\langle \mathbf{R}, JM | H | \mathbf{R}', J'M' \rangle = \sum_{\alpha,\alpha',\sigma} C^{*}(\alpha\sigma; JM) \times C(\alpha'\sigma; J'M') \times \langle \mathbf{R}\alpha | H | \mathbf{R}'\alpha' \rangle$$

Nair,Ramaniah,Rustagi PRB 45,5969(1992)

USE SYMMETRY TO REDUCE MATRIX SIZE

FORM LINEAR COMBINATIONS THAT TRANSFORM LIKE IRREDUCIBLE REPRESENTATIONS OF TETRAHEDRAL GROUP

$$\sum_{n,i,\nu} C_n^{i\nu}\, u_{\nu}^{\Gamma_i}(R_n)$$

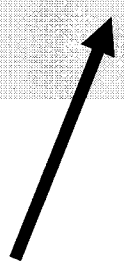

n th component of Γ_i irreducible representation

FITTING PARAMETERS NEAR ZONE CENTER

$$H_{\alpha\alpha'}(\mathbf{k}) = [(E_p + 8E_{xx} + 4E_{zz}) - (E_{xx} + E_{zz})k^2a^2/2 + (E_{zz} - E_{xx})k_\alpha^2 a^2/2]\delta_{\alpha\alpha'} + (-E_{xy}k_\alpha k_{\alpha'}a^2)(1 - \delta_{\alpha\alpha'}) .$$

TABLE II. Tight-binding parameters for VBM and CVBM, which reproduce band structure close to the Γ point accurately. $\mathcal{E}_0 = \hbar^2/2m_0a^2$.

VBM	CVBM
$E_p = E_v - 12\gamma_1\mathcal{E}_0$	$E_{xx} = (\gamma_1 - 2\gamma_2)\mathcal{E}_0 + X_{\text{LH-SO}}/16$
$E_{xx} = (\gamma_1 + 4\gamma_2)\mathcal{E}_0$	$E_{zz} = (\gamma_1 - 2\gamma_2)\mathcal{E}_0 - X_{\text{LH-SO}}/16$
$E_{zz} = (\gamma_1 - 8\gamma_2)\mathcal{E}_0$	$E_{sx}^2 = E_g/8[(\gamma_1 + \gamma_2)\mathcal{E}_0 - (3E_{xx} + E_{zz})/4]$
$E_{xy} = 6\gamma_3\mathcal{E}_0$	$E_{xy} = 6\gamma_3\mathcal{E}_0 + 16E_{sx}^2/E_g$
	$E_s = E_c + 12\hbar^2/2m_e - 64E_{sx}^2[2/E_g + 1/(E_g + \Delta)]$
	$E_{ss} = -\hbar^2/2m_e + [2/E_g + 1/(E_g + \Delta)]16E_{sx}^2/3$
	$E_p = E_v - (8E_{xx} + 4E_{zz})$

Nair,Ramaniah,Rustagi PRB 45,5969(1992)

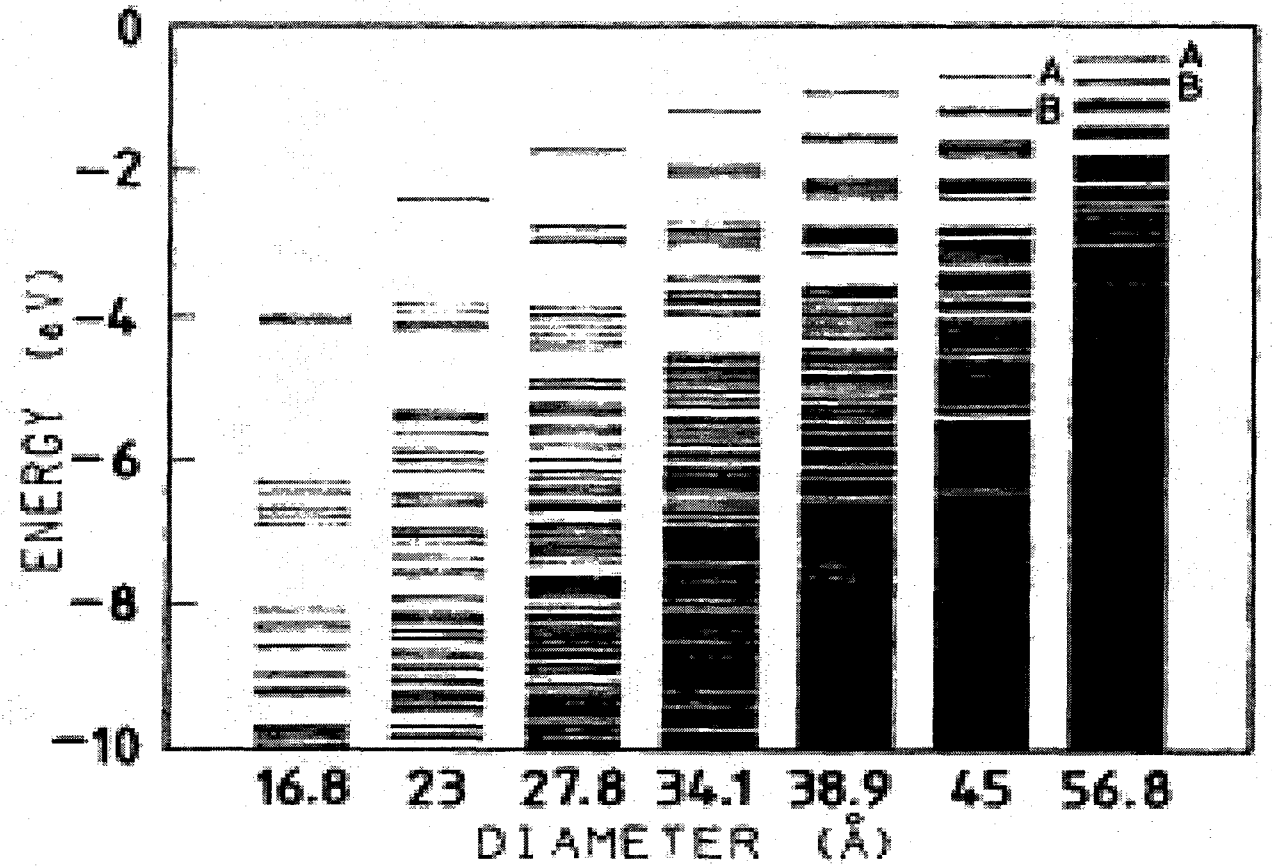

FIG. 2. The energy levels of GaAs crystallites calculated using the VBM with parameters obtained by fitting the Γ-point masses. The results for seven different crystallite sizes ranging from 16.8 to 56.8 Å diameter are shown. The zero of the energy scale is at the bulk valence-band edge.

Nair,Ramaniah,Rustagi PRB 45,5969(1992)

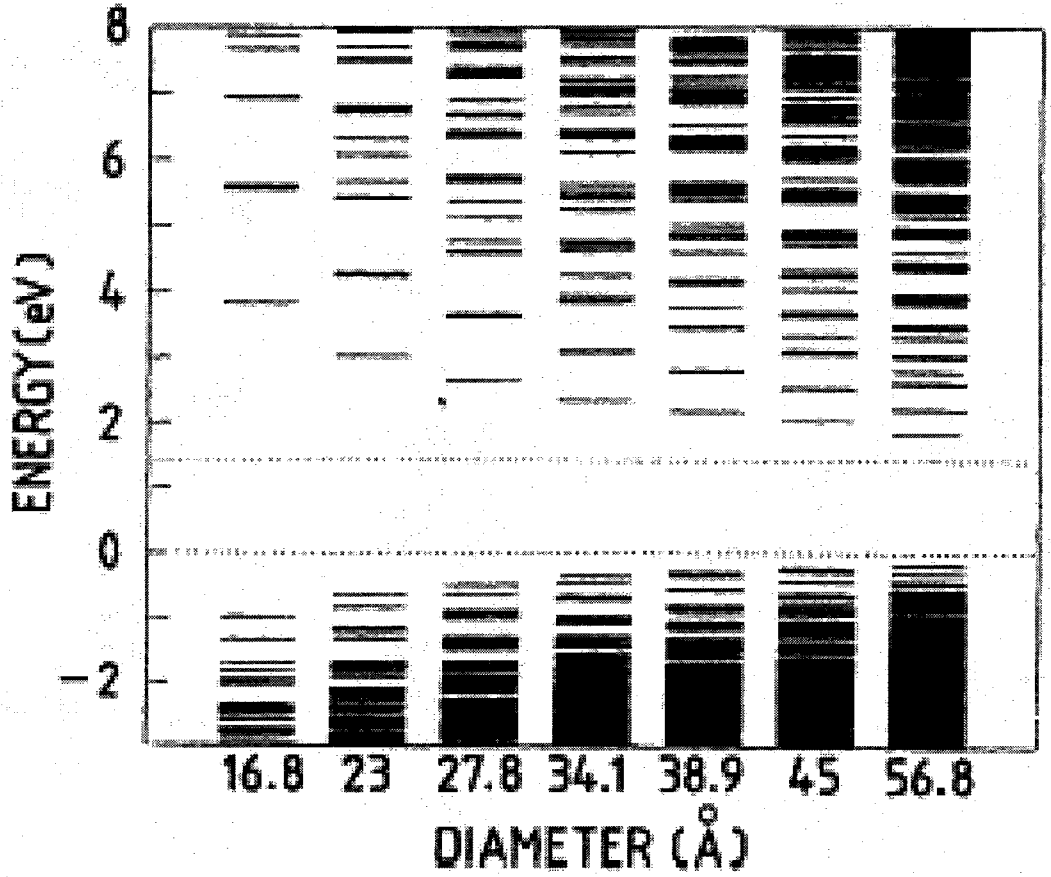

FIG. 4. The electron- and hole-energy levels of GaAs crystallites given by CVBM. The positions of the bulk valence- and conduction-band edges are indicated by dotted lines.

Nair,Ramaniah,Rustagi PRB 45,5969(1992)

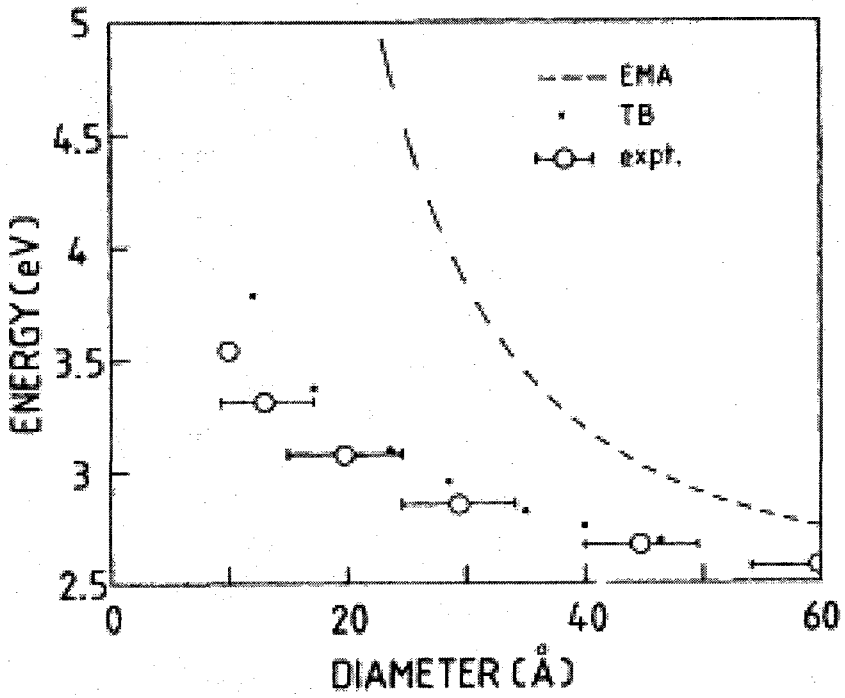

FIG. 9. The size dependence of the exciton position in CdS crystallites. The dots represent the result of a tight-binding calculation using CVBM. The dashed line is given by an effective-mass calculation using a three-band model for the valence band and a single-band model for the conduction band. The open circles represent experimental data (Ref. 7).

Nair,Ramaniah,Rustagi PRB 45,5969(1992)

TABLE I. The confinement energies (in eV) for a few topmost valence-band levels in CdS quantum dots. The symmetry of each level is also indicated.

Diameter (Å)	One-band EMA	Multiband EMA	Tight-binding (EBOM)
70	0.038	0.076 (Γ_8^+)	0.07 (Γ_8^+)
		0.106 (Γ_6^+)	
		0.091 (Γ_8^-)	
		0.139 (Γ_7^-)	
38	0.130	0.236 (Γ_8^+)	0.19 (Γ_8^+)
		0.266 (Γ_6^+)	0.22 (Γ_6^+)
		0.299 (Γ_8^-)	0.20 (Γ_8^-)
		0.347 (Γ_7^-)	0.25 (Γ_7^-)
24	0.326	0.576 (Γ_8^+)	0.43 (Γ_8^+)
		0.606 (Γ_6^+)	0.46 (Γ_6^+)
		0.743 (Γ_8^-)	0.41 (Γ_8^-)
		0.791 (Γ_7^-)	0.46 (Γ_7^-)

Refs: Colvin et al PRL 66,2786(1991), Nair et al PRL 68,893(1992)

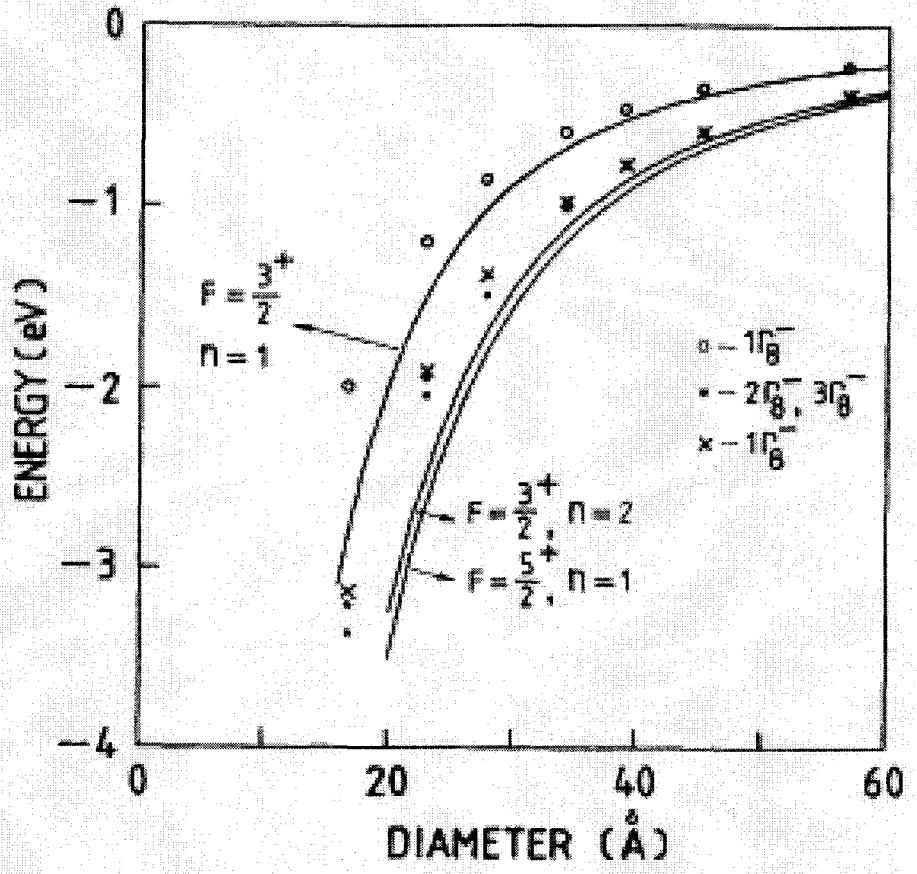

FIG. 3. The size dependence of a few topmost valence-band levels (circles, crosses, and dots) in GaAs crystallites obtained using VBM. The solid lines represent the corresponding results given by a multiband effective mass calculation. The notation $n\Gamma_v^{\pm}$ stands for the nth level of $\Gamma_v^{\pm}$ symmetry.

Nair,Ramaniah,Rustagi PRB 45,5969(1992)

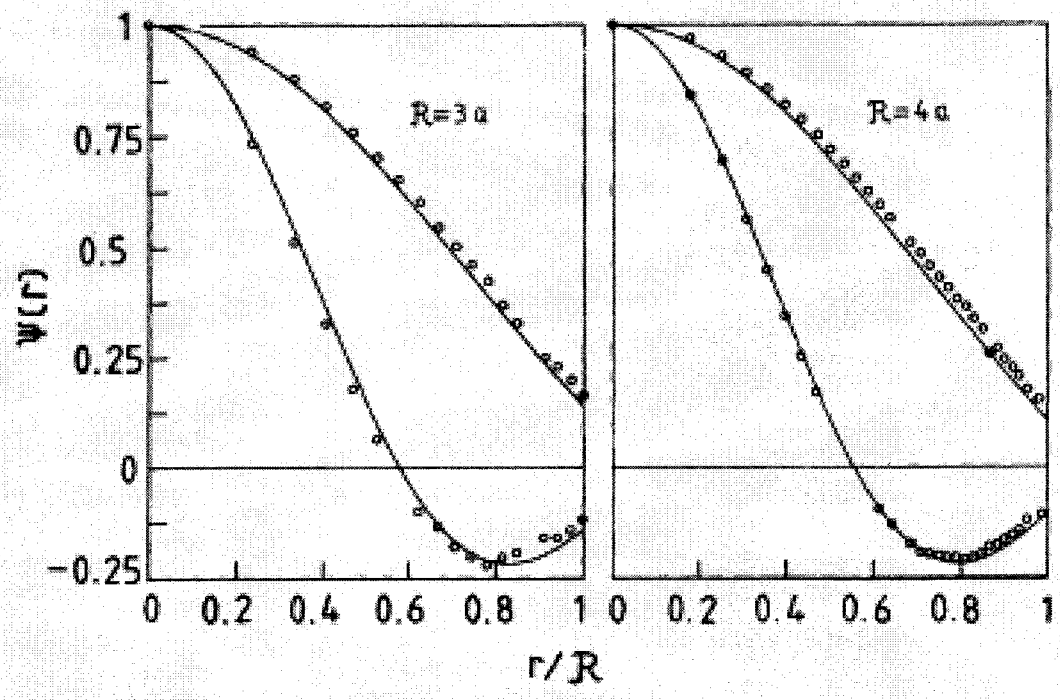

FIG. 6. The lowest two $l=0$ EMA envelope functions for the conduction band obtained using a single parabolic band model with a confining potential of 10 eV (solid line) compared with the corresponding wave function given by CVBM for GaAs crystallites (open circles). The results for two crystallite sizes are shown.

Nair,Ramaniah,Rustagi PRB 45,5969(1992)

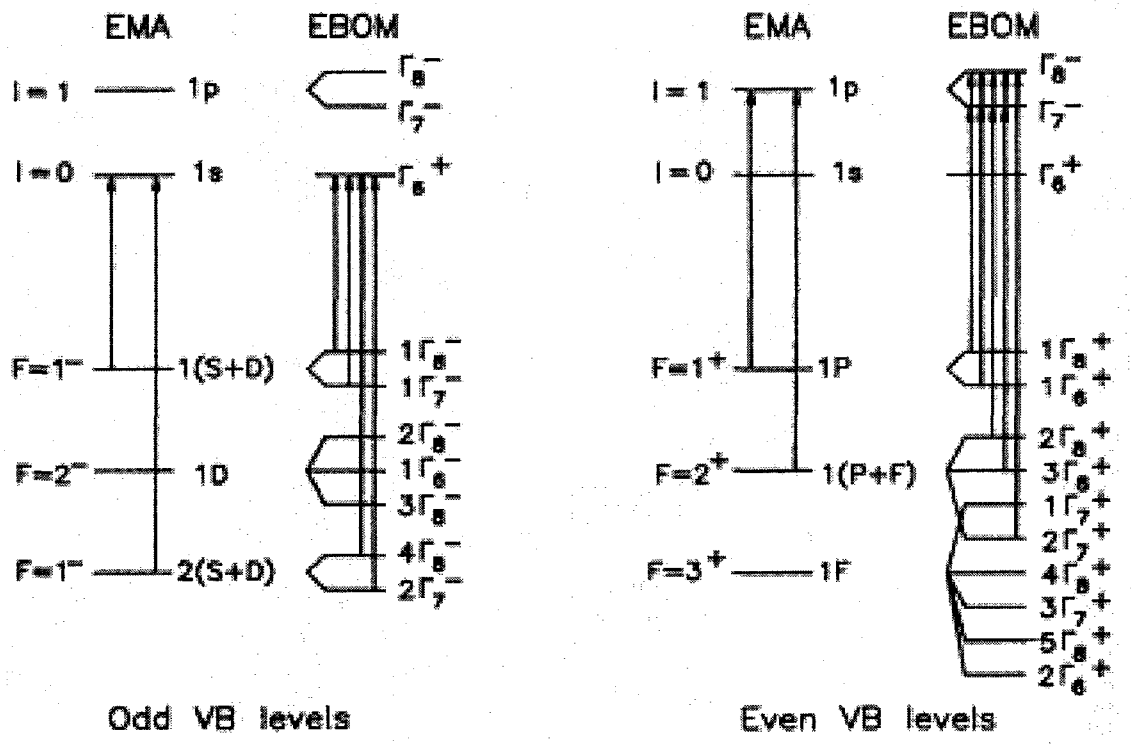

FIG. 1. Correspondence between the qualitative level structure of the near-band-edge energy levels obtained using the EBOM and the EMA, for CdS QD's. In the EMA, a three-band model for the valence band (VB) and a single-band model for the conduction band (CB) have been used. The interband transitions, allowed according to the EMA selection rules, are also indicated.

Ramaniah & Nair PRB(1993)

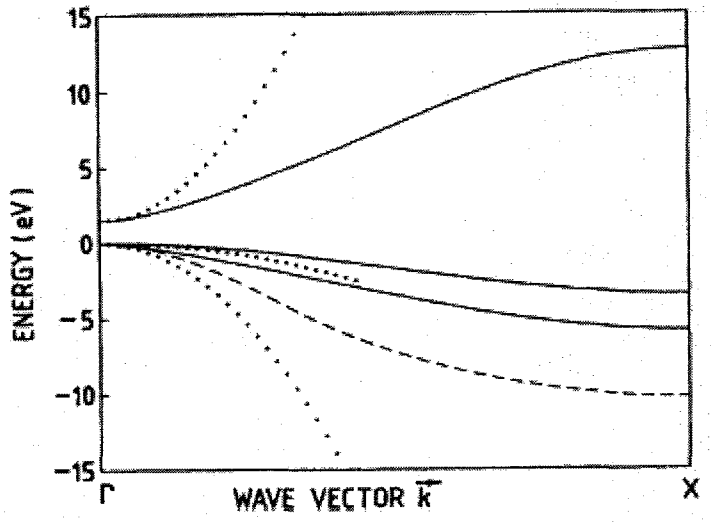

FIG. 1. The calculated band structure of the valence and conduction bands for GaAs along the Γ-X direction using an effective bond-orbital model with parameters obtained by fitting the bulk Γ-point masses. The dashed lines are obtained in a valence-band model (VBM), while the solid lines are given by the CVBM which includes a conduction-band orbital also; both give identical dispersions for the heavy-hole band. The parabolic dispersions given by the band-edge masses are also shown (dotted lines).

Nair,Ramaniah,Rustagi PRB 45,5969(1992)

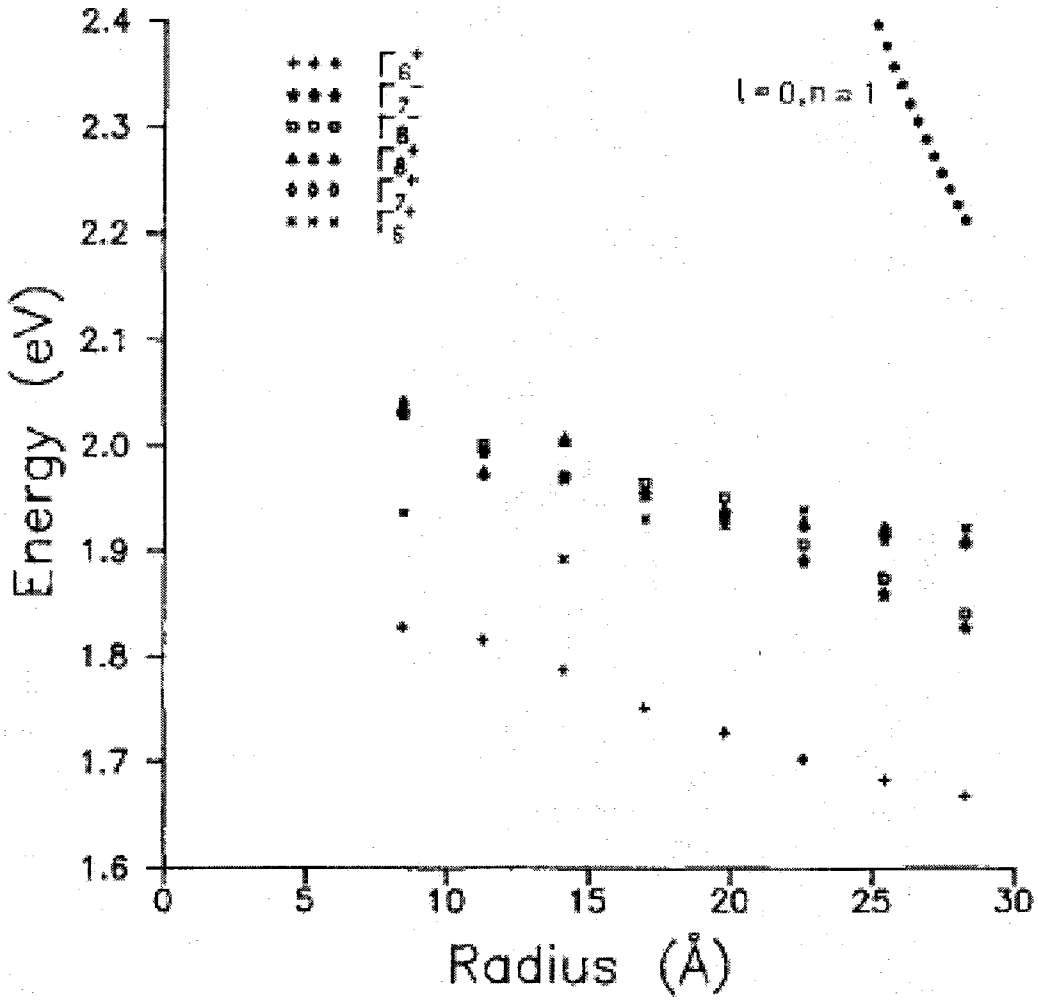

Fig. 2. The size dependence of the first six CB levels (pluses, stars, squares, triangles, diamonds, and crosses) in GaAs QDs, calculated within the effective-bond-orbital-model. The $l = 0$, $n = 1$ level predicted by a single band effective mass approximation is also shown.

Ramaniah & Nair, PhysicaB212,245 (1995)

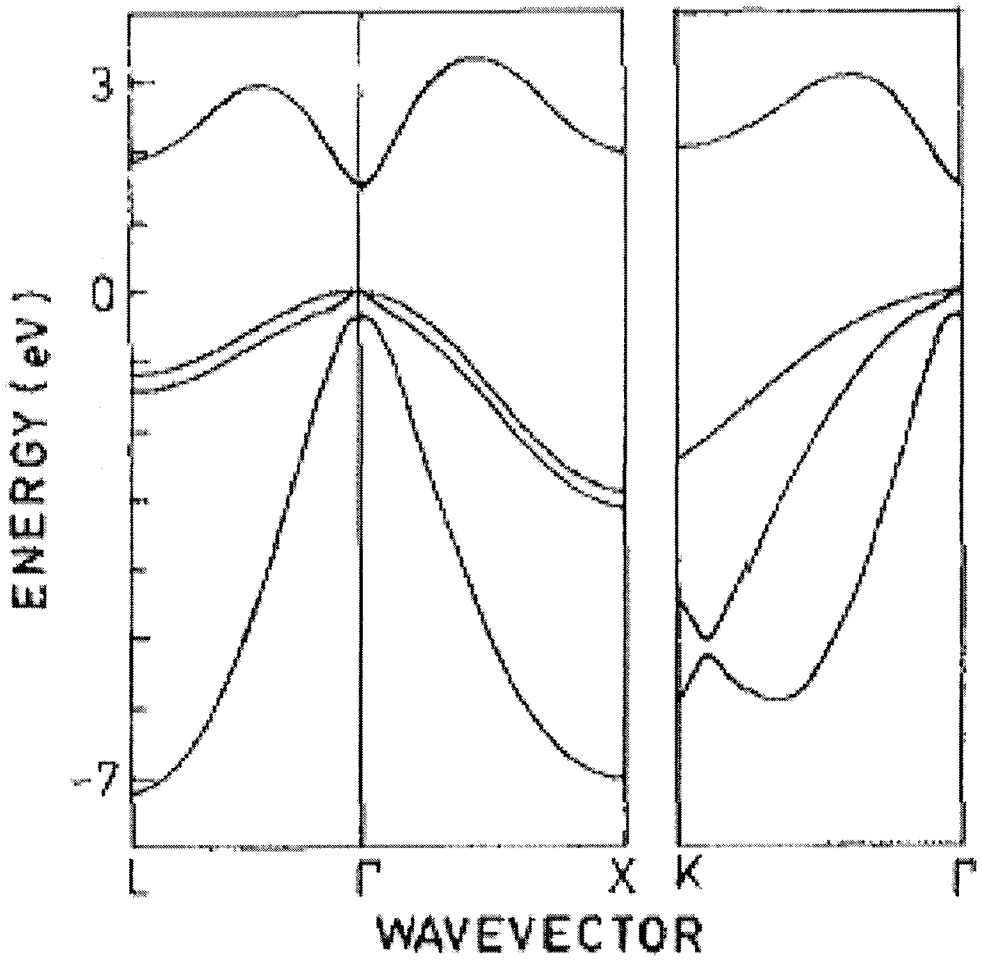

Fig. 1. The bulk band structure of cubic GaAs obtained using the effective-bond-orbital-model.

Ramaniah & Nair, PhysicaB212,245 (1995)

SELECTION RULES

band index,

$$\Psi = \sum_b \int d\vec{k} A^b(\vec{k}) e^{i\vec{k}.\vec{r}} u_{b\vec{k}}(\vec{r})$$

$$[\varepsilon(-i\vec{\nabla}) + U(\vec{r})]F_n(\vec{r}) = \varepsilon_n F_n(\vec{r})$$

$$F_n(\vec{r}) = \int e^{i\vec{k}.\vec{r}} A_n(\vec{k}) d\vec{k}$$

$$F_{nlm}(\vec{r}) = \frac{\sqrt{2}}{R^{3/2}} \frac{1}{j_{l+1}(\zeta_{nl})} j_l\left(\zeta_{nl} \frac{r}{R}\right) \mathrm{Y}_{lm}(\theta, \phi)$$

$$\langle vnlm|\vec{p}|cn'l'm'\rangle =$$

$$\sum_{kk'}\sum_{\vec{R}_l} A^{*}_{nlm}(\vec{k})A_{n'l'm'}(\vec{k}')e^{i(\vec{k}'-\vec{k}).\vec{R}_l}$$

$$\int_{cell} u^{*}_{v\vec{k}}(\vec{r})(\hbar\vec{k}'+\vec{p})u_{c\vec{k}'}(\vec{r})e^{i(\vec{k}'-\vec{k}).\vec{r}}d\vec{r}$$

FOR INFINITE SOLIDS

$$\sum_{\vec{R}_l} e^{i(\vec{k}'-\vec{k}).\vec{R}_l} = \delta_{\vec{k},\vec{k}'}$$

FOR QD CORRECTIONS ~ a/R

$$\langle vnlm|\vec{p}|cn'l'm'\rangle \approx \vec{p}_{cv}(0)\delta_{nlm,n'l'm'}$$

IF $\vec{p}_{cv}(0) = 0$

$$\langle vnlm|\vec{p}|cn'l'm'\rangle = M_{cv}^{\mu\nu} \int F_{nlm}(\vec{r})\vec{p}F_{n'l'm'}(\vec{r})d\vec{r}$$

$$M_{cv}^{\mu\nu} = \frac{1}{\hbar}\frac{\partial \vec{p}_{cv}^{\mu}(\vec{k})}{\partial \vec{k}^{\nu}}\bigg|_{k=0}$$

~1/R

Transition Rate ~ 1/R²

Alka Ingale, Kavita Borgohain, Shailaja Mahamuni and K.C. Rustagi(unpublished)

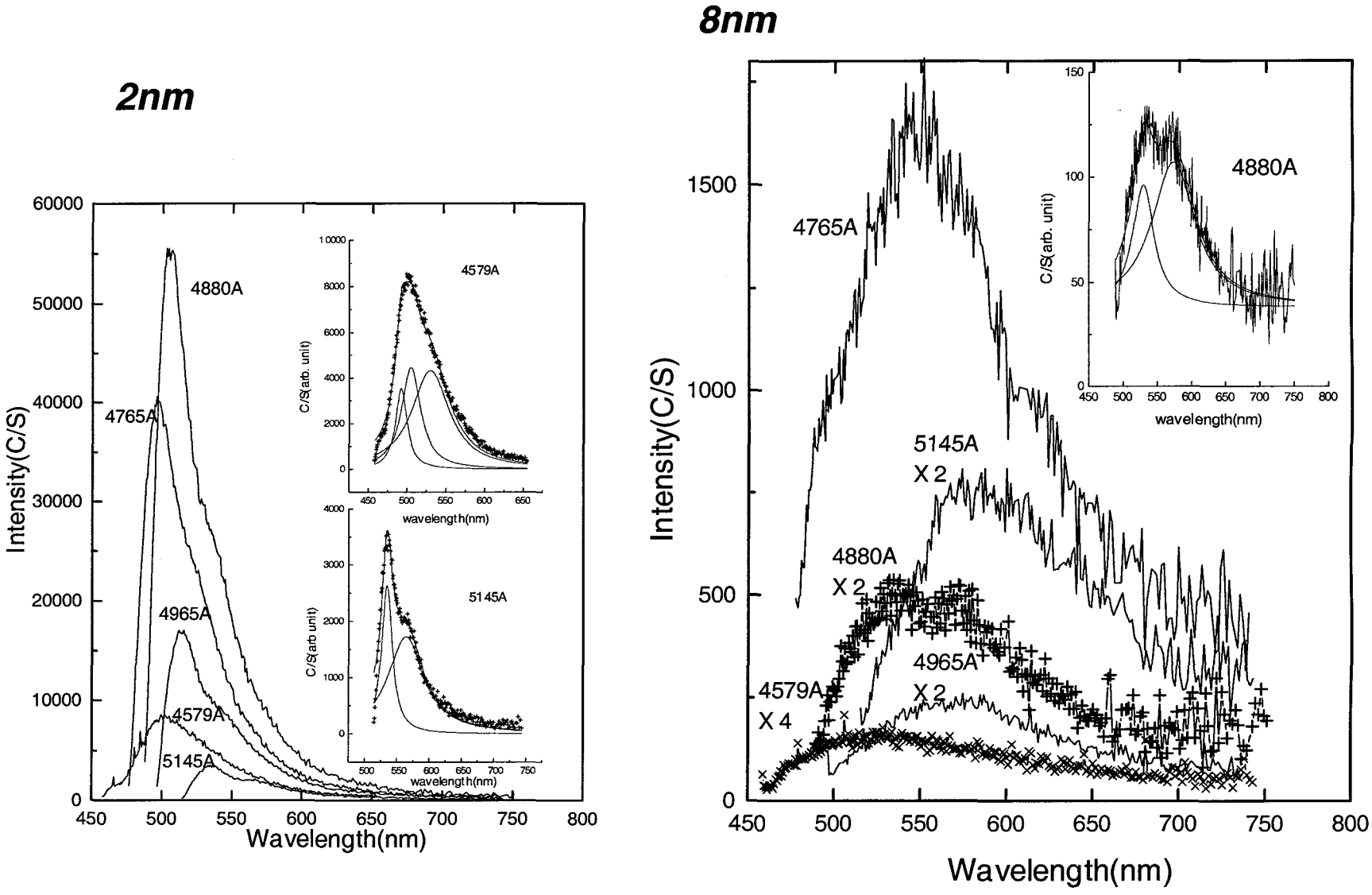

Alka Ingale, Kavita Borgohain, Shailaja Mahamuni and K.C. Rustagi(unpublished)

structural changes also change energy levels!

PHYSICAL REVIEW B 71, 045318 (2005)

Cylindrically shaped zinc-blende semiconductor quantum dots do not have cylindrical symmetry: Atomistic symmetry, atomic relaxation, and piezoelectric effects

Gabriel Bester and Alex Zunger
National Renewable Energy Laboratory, Golden, Colorado 80401, USA
(Received 1 April 2004; published 14 January 2005)

Self-assembled quantum dots are often modeled by continuum models (effective mass or $\mathbf{k}\cdot\mathbf{p}$) that assume the symmetry of the dot to be that of its overall geometric shape. Lens-shaped or conical dots are thus assumed to have continuous cylindrical symmetry $C_{\infty v}$, whereas pyramidal dots are assumed to have C_{4v} symmetry. However, considering that the III–V dots are made of atoms arranged on the (relaxed) positions of a zinc-blende lattice, one would expect the highest possible symmetry in these structures to be C_{2v}. In this symmetry group all states are singly degenerate and there are no *a priori* reason to expect, e.g., the electron P states (usually the second and third electron levels of dominant orbital P character) to be degenerate. Continuum models, however, predict these states to be energetically degenerate unless an irregular shape is postulated. We show that, in fact, the true (atomistic) symmetry of the dots is revealed when the effects of (i) interfacial symmetry, (ii) atomistic strain, and (iii) piezoelectricity are taken into account. We quantify the contributions of each of these effects separately by calculating the splitting of electron P levels for different dot shapes at different levels of theory. We find that for an ideal square-based pyramidal InAs/GaAs dot the interfacial symmetry of the unrelaxed dot splits the P level by 3.9 meV, atomistic relaxation adds a splitting of 18.3 meV (zero if continuum elasticity is used to calculate strain) and piezoelectricity reduces the splitting by −8.4 meV, for a total splitting of 13.8 meV. We further show that the atomistic effects (i) and (ii) favor an orientation of the electron wave functions along the $[1\bar{1}0]$ direction while effect (iii) favors the [110] direction. Whereas effects (i) + (ii) prevail for a pyramidal dot, for a lens shaped dot, effect (iii) is dominant. We show that the 8–band $\mathbf{k}\cdot\mathbf{p}$ method, applied to pyramidal InAs/GaAs dots describes incorrectly the splitting and order of P levels (–9 meV instead of 14 meV splitting) and yields the orientation [110] instead of $[1\bar{1}0]$.

ENVELOPE FUNCTIONS FOR OTHER SHAPES

B.Lamprecht *etal*

Appl Phys.B68,419(1999)

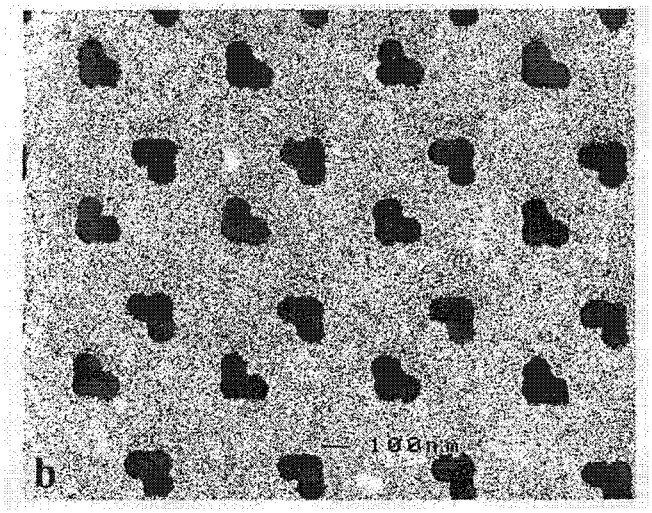

SHG(>>) ~ 40SHG(<>)

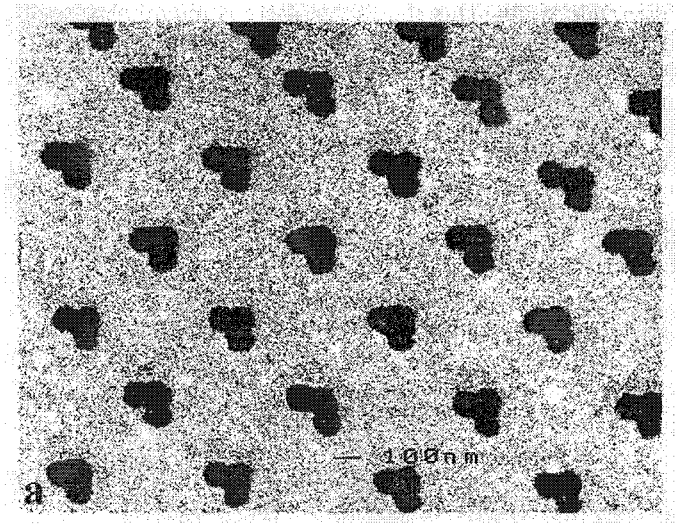

METAL NANOPARTICLES

Third harmonic generation in metals was measured by Burns and Bloembergen in 1969

Theory? Free particle nonlinearity negligible

Surface? Collisions? Higher order multipoles?

In nano particles: $\chi^{(3)}_{\text{eff}} = \chi^{(3)}_{\text{metal}} f^2 |f|^2$

$\chi^{(3)}_{\text{metal}} = ???$

Size quantization main cause of nonlinearity

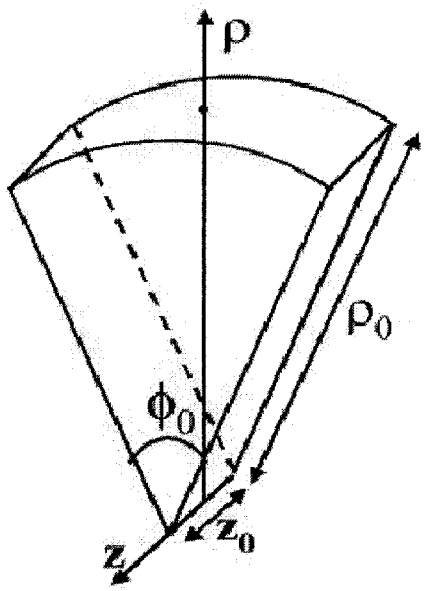

Easy solutions for apex angle=π/integer(X)

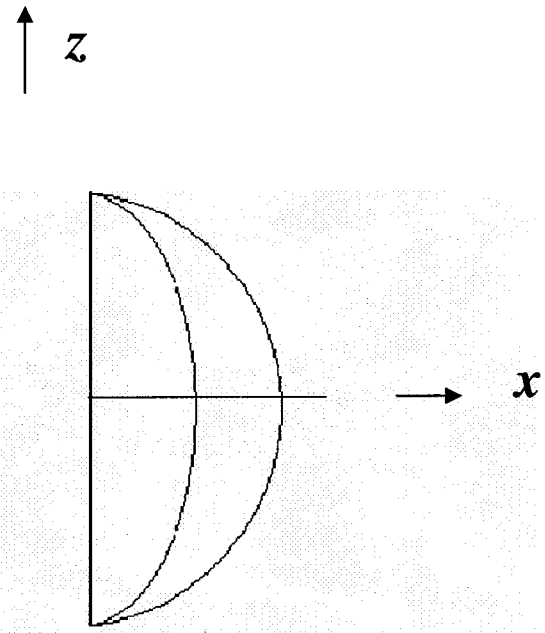

X=1 means hemisphere

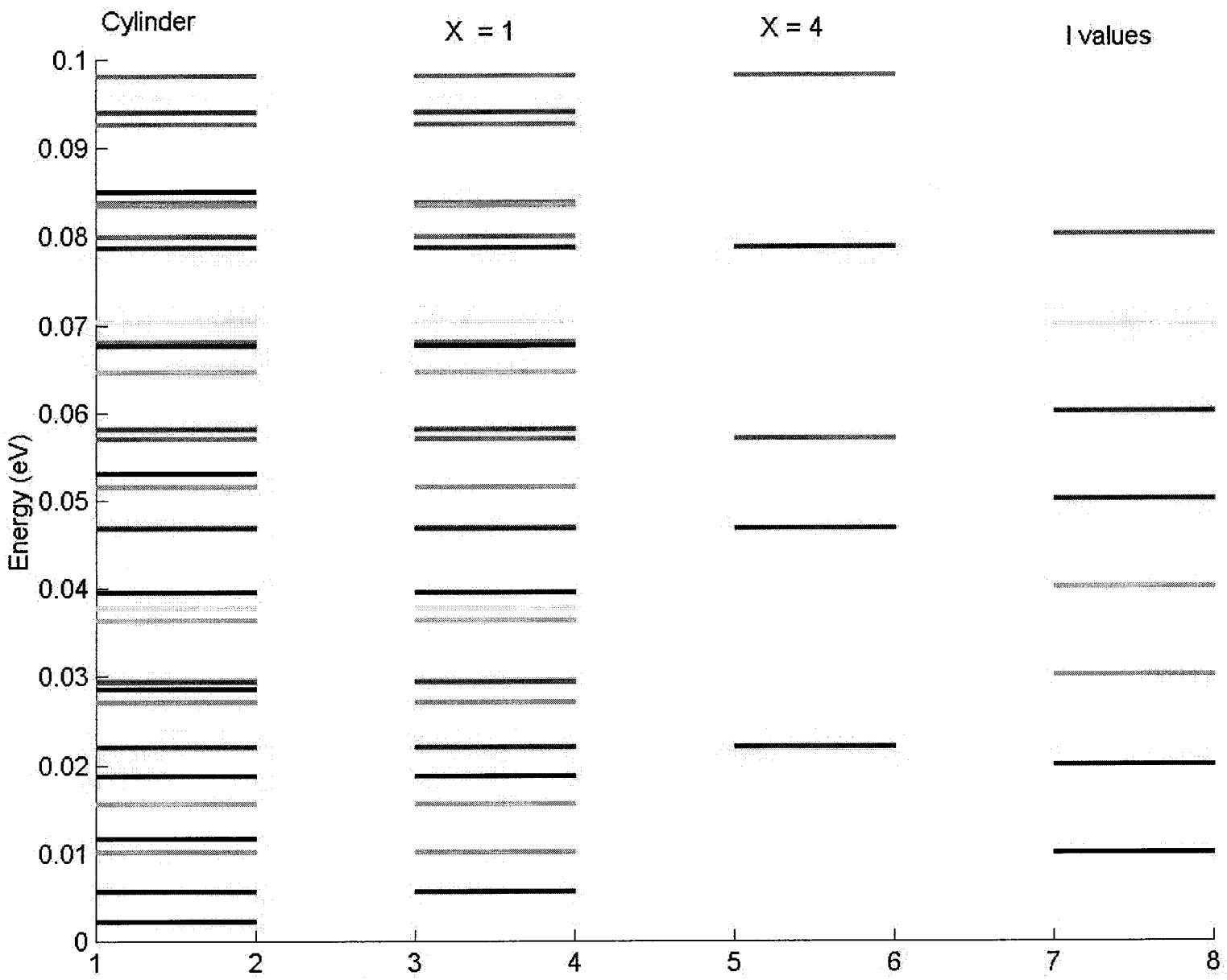
Cylinder
X = 1
X = 4
l values
Energy (eV)
0.1
0.09
0.08
0.07
0.06
0.05
0.04
0.03
0.02
0.01
0
1
2
3
4
5
6
7
8

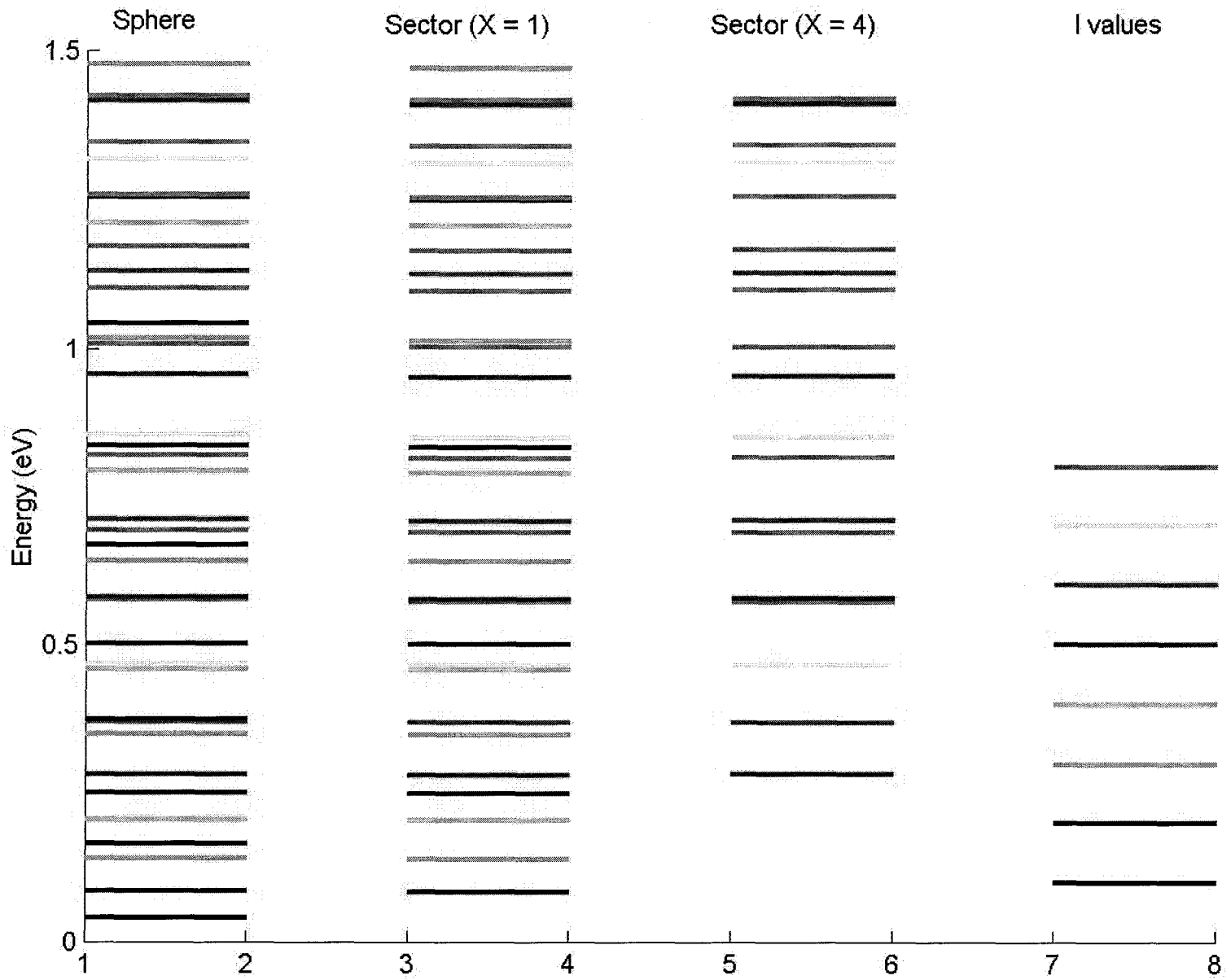
Sphere
Sector (X = 1)
Sector (X = 4)
l values
Energy (eV)
1.5
1
0.5
0
1
2
3
4
5
6
7
8

Spherical Quantum Dot

$$\psi_{nlm}(r,\theta,\phi) = \frac{2^{1/2}}{R^{3/2}} \frac{1}{j_{l+1}(\varsigma_{nl})} j_l\left(\varsigma_{nl}\frac{r}{R}\right) Y_{lm}(\theta,\phi),$$

$$E_0 = \frac{\hbar^2}{2m^* R^2}\varsigma_{nl}^2$$

ς_{nl} zeros of the spherical Bessel function.

Hemispherical Quantum Dot:

Out of these solutions,select those which vanish at z=0 plane

Lowest state *l*=1

For same volume :

hemispherical QD has larger confinement energy

Effect of electron-electron interaction

Dielectric Confinement

Screening -- depolarization field,
sensitive to shape
plasmon resonance -Correlated motion :
beyond single particle picture

Generalized Kohn Theorem

Interacting electrons in Harmonic oscillator potential absorb only at ω_0

Screened γ = single particle γ . local field factor

$$f_x(\omega) = \frac{1}{1 + L_x(\varepsilon_{xx} - 1)}$$

$$L_x = \frac{abc}{3}\int_0^\infty \frac{dq}{(a^2+q^2)^{3/2}(b^2+q^2)^{1/2}(c^2+q^2)^{1/2}}$$

For long molecules: $L_x \rightarrow 0$

Jayabalan etal PRB (2003)

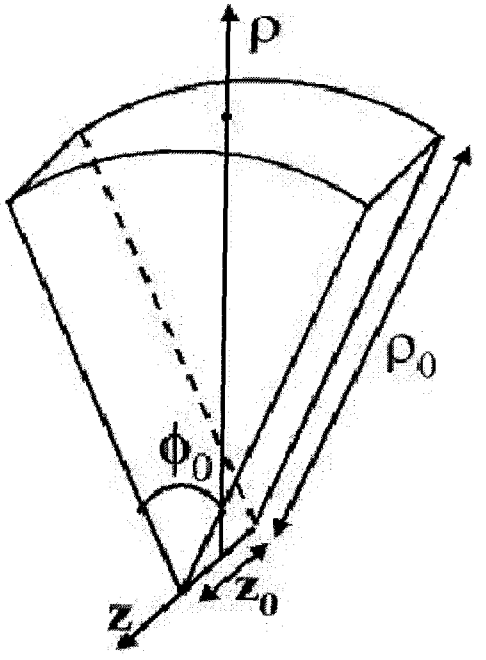

$$\phi_0 = \frac{\pi}{X},$$ X integer

$$\Psi_{\nu,n,s} = \frac{1}{\sqrt{z_0}} \sin\left(\frac{\nu\pi}{z_0}(z + z_0/2)\right)\psi_{ns}(\rho,\phi),$$

$$\nu = 1, 2, 3, \ldots,$$

$$\psi_{ns}(\rho,\phi) = \frac{2}{\rho_0}\sqrt{\frac{X}{\pi}}\frac{1}{J_{Xn+1}(\alpha_{ns})} J_{Xn}\left(\alpha_{ns}\frac{\rho}{\rho_0}\right)\zeta_n(\phi),$$

α_{ns} zeros of the Bessel function.

$$n = 1,2,3,\ldots,$$

$$s = 1,2,\ldots,$$

$$E_{\nu ns} = \alpha_{ns}^2 E_0 + \nu^2 E_z, \quad E_z = \frac{\hbar^2\pi^2}{2mz_0^2}. \quad E_0 = \frac{\hbar^2}{2m\rho_0^2}$$

Electronic density

Jayabalan etal PRB (2003)

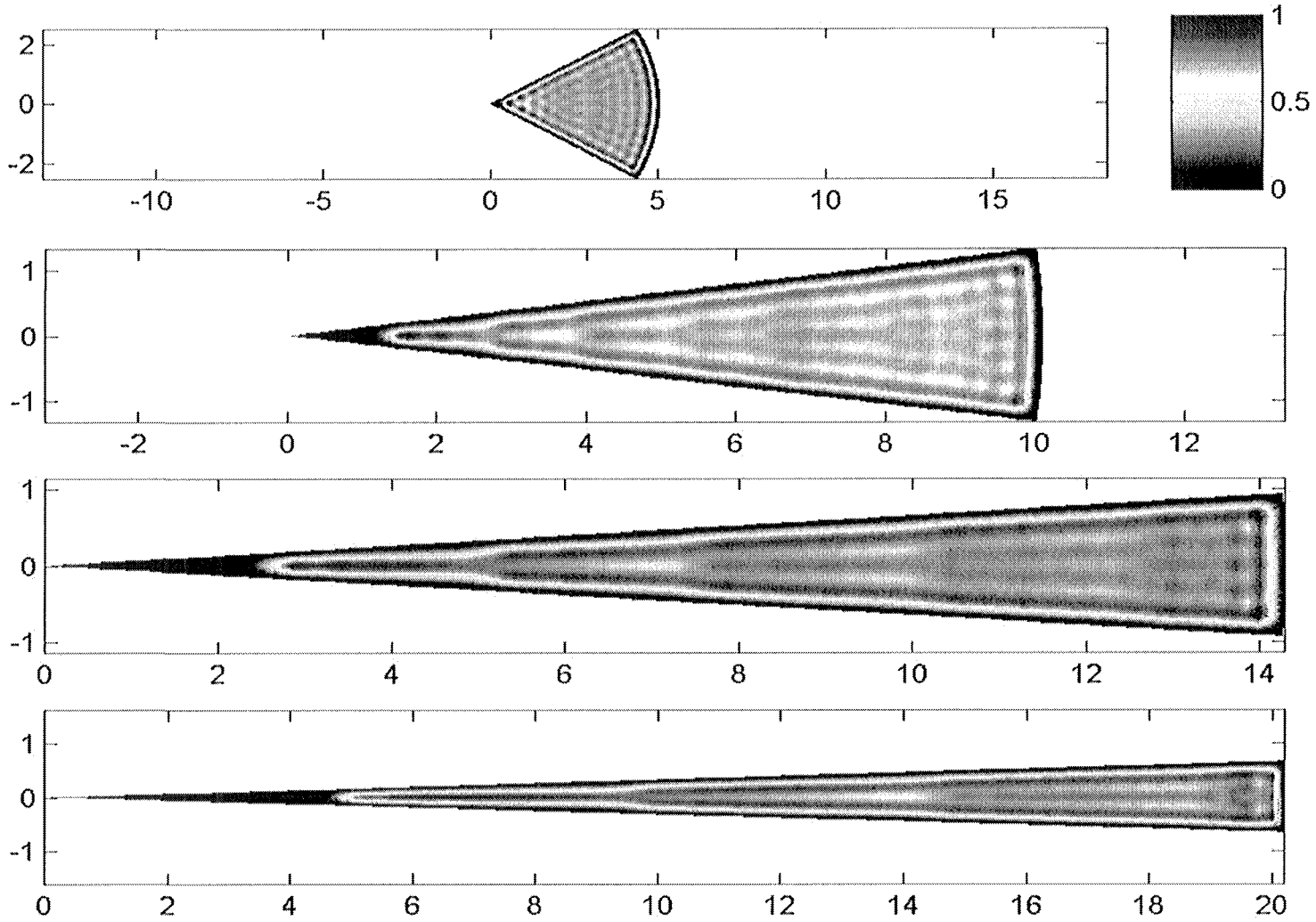

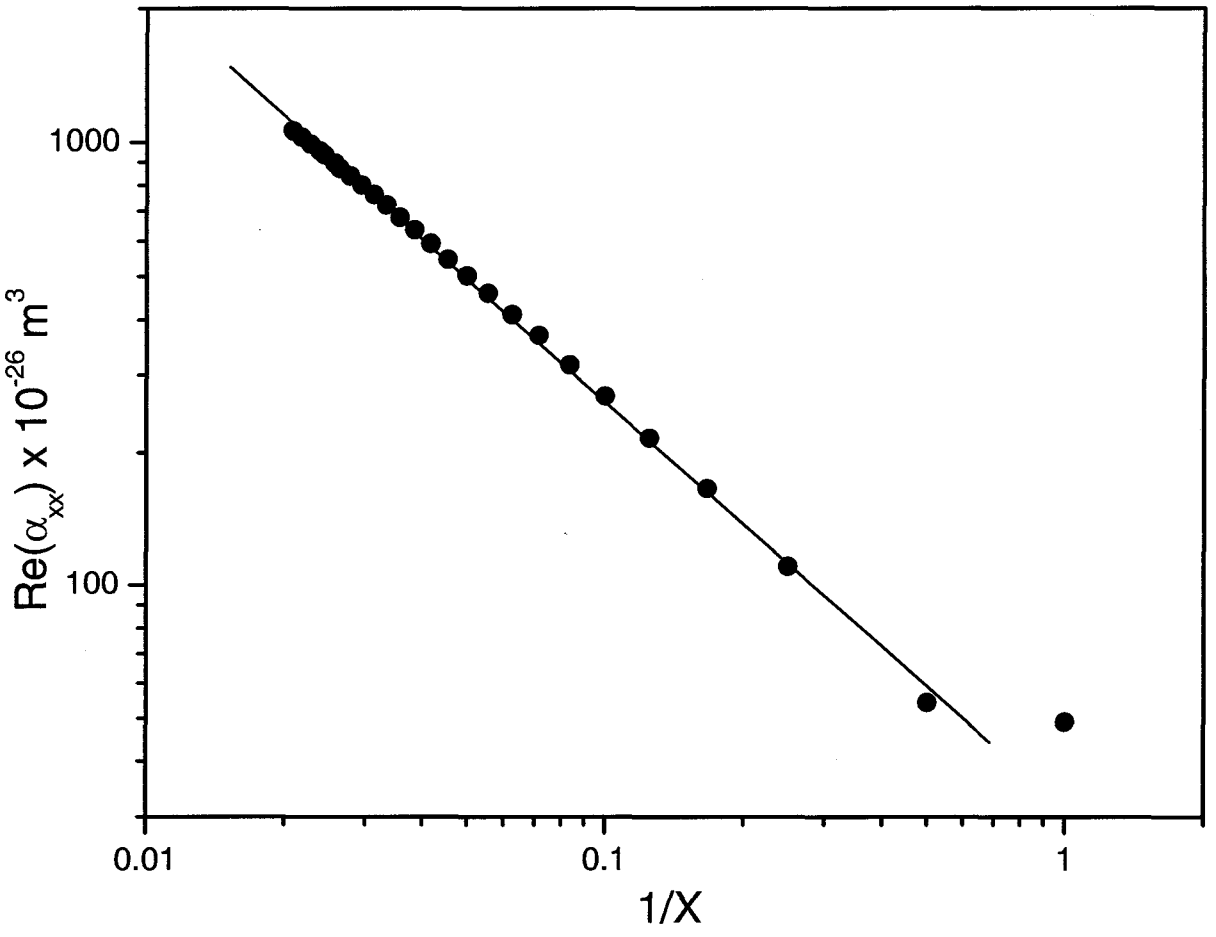

Jayabalan etal PRB (2003)

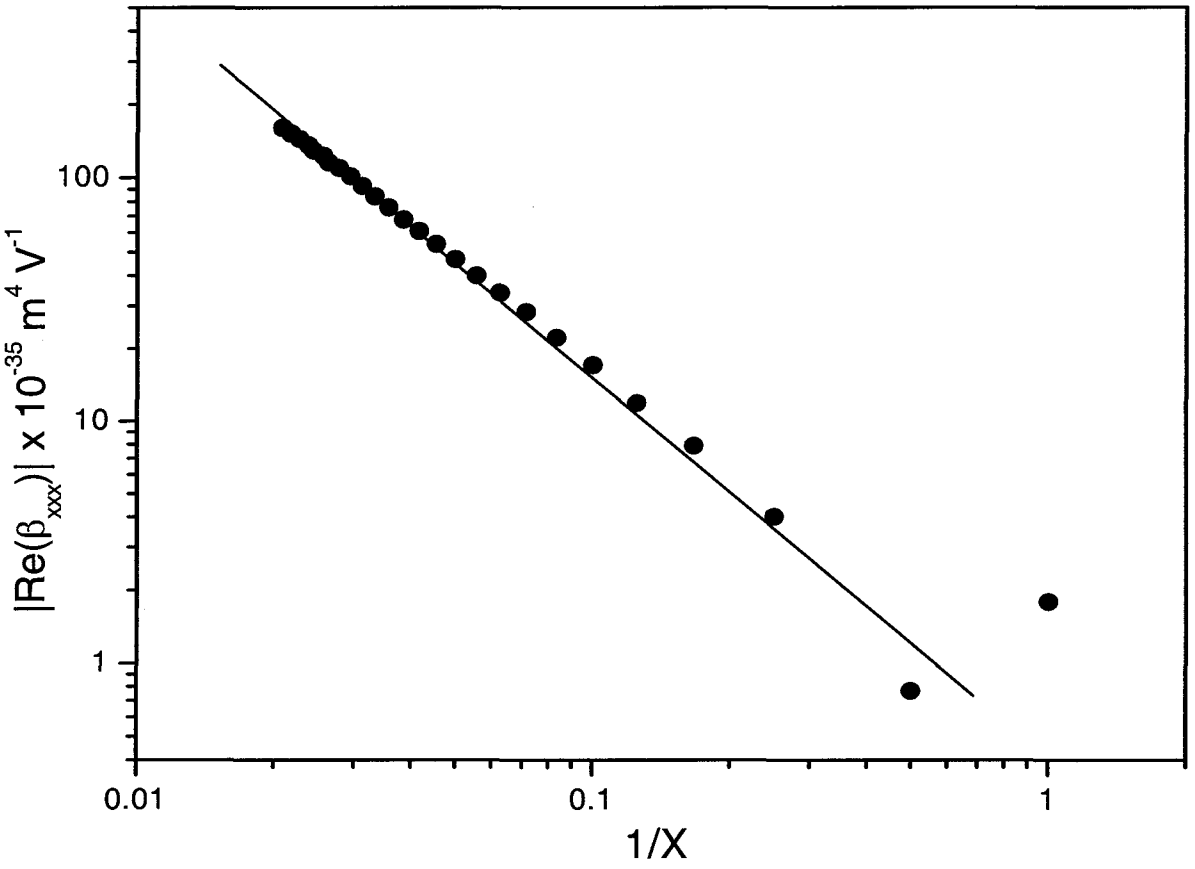

Jayabalan etal PR B (2003)

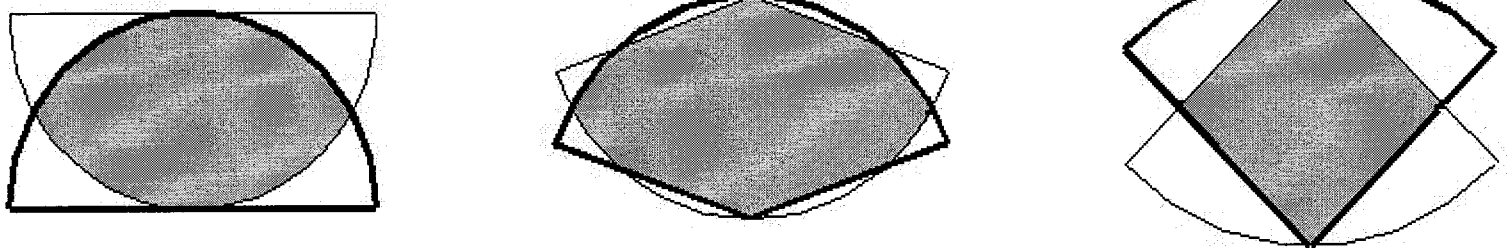

(a) (b) (c)

Jayabalan etal PR B(2003)

EXCITONS

Exciton wave function has the form:

$$\Psi(r_1, r_2) = \psi(r_1, r_2) u_c(r_1) u_v(r_2)$$

Envelope function varies slowly and obeys wave equation:

$$\left[-\frac{\hbar^2 \nabla_1^2}{2m_1} - \frac{\hbar^2 \nabla_2^2}{2m_2} - \frac{e^2}{4\pi\epsilon_0 \epsilon r_{12}} + V_0 \right] \psi(\mathbf{r}_1, \mathbf{r}_2) = E\psi(\mathbf{r}_1, \mathbf{r}_2) ,$$

With boundary condition:

$$\psi(\mathbf{r}_1, \mathbf{r}_2) = 0 \quad \text{for } r_1 \text{ or } r_2 \geq R .$$

Nair,Sinha,Rustagi PRB (1987)

LIMITING CASES(Efros & Efros(1982))

Strong confinement Confinement energy<coulomb energy

Weak confinement: Confinement energy<coulomb energy

Exciton with quantized center of mass motion

$$E = E_g + E_{ex} + \frac{\hbar^2 \pi^2}{2MR^2}$$

$$\psi \sim \frac{\sin(\pi r_{\text{c.m.}}/R)}{r_{\text{c.m.}}/R} e^{-r_{12}/a_0},$$

Not compatible with boundary conditions

Strong confinement

Confinement energy >> coulomb energy

electron and hole motion quantized

Coulomb interaction treated perturbatively

(Efros & Efros(1982))

$$E = E_g + E_{ex} + \frac{\hbar^2 \pi^2}{2\mu R^2} - 1.786\frac{e^2}{\varepsilon R} - 0.248\frac{\mu e^4}{2\varepsilon^2 \hbar^2}$$

Nair et al PRB(1987)

Nair et al PRB(1987)

Variational calculation with trial wave function:

$$\psi(\mathbf{r}_1,\mathbf{r}_2)=\begin{cases} N\left|\dfrac{\sin(\pi r_1/R)}{r_1/R}\right|^{\alpha_1}\left|\dfrac{\sin(\pi r_2/R)}{r_2/R}\right|^{\alpha_2}\exp(-\beta r_{12}/R) & \text{for } r_1,r_2\le R \\ 0 \quad \text{outside,} \end{cases}$$

Centre of mass quantization?

$$E = E_g + E_{ex} + \frac{\hbar^2\pi^2}{2M(R+d)^2}$$

See Also Kayanuma SSC (1986),PRB (1988)

Nair et al PRB(1987) CdS:

------ one parameter calc.

_____ 3 parameters calc

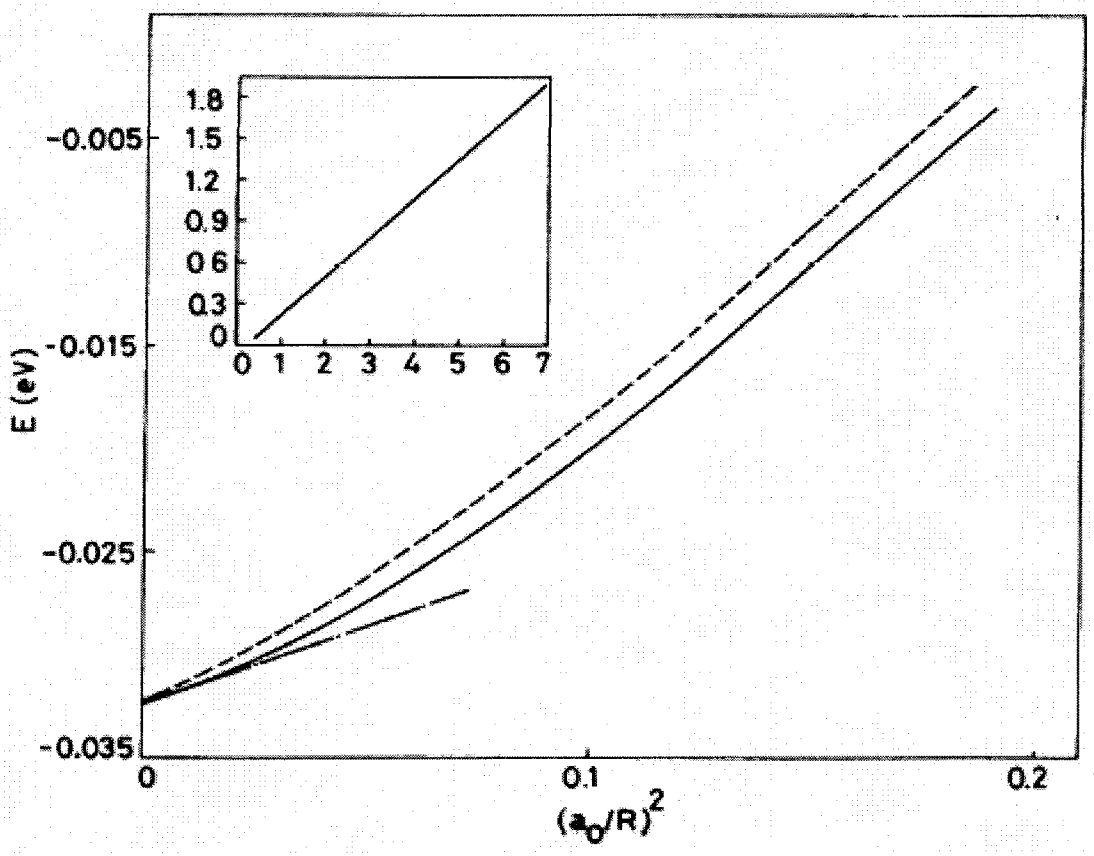

Nair et al PRB(1987) CuCl

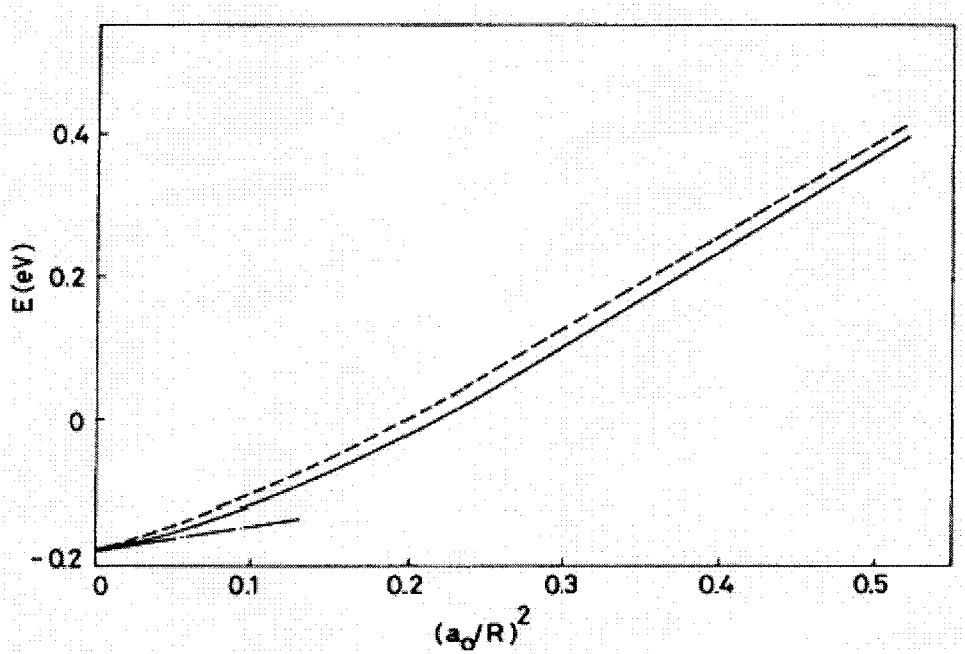

Biexcitons in Quantum dots and nonlinear response

Nair and Takagahara PRB 55,5153(1997)

$$\psi_0(\mathbf{r}_e,\mathbf{r}_h)=\sum_{l=0}^{l_{\max}}\sum_{m=0}^{m_{\max}}\sum_{n=0}^{n_{\max}} c_{lmn}\, w_m(r_e)\, w_n(r_h)\, r_{\mathrm{eh}}^{l} \times \exp(-r_{\mathrm{eh}}/a_{\mathrm{ex}}) \qquad w_m(r)=\prod_{k=1}^{m}\left[r^2-\left[\frac{k}{m}R\right]^2\right]$$

$$H_{xx}=-\frac{\hbar^2}{2m_e}(\nabla_{e_1}^2+\nabla_{e_2}^2)-\frac{\hbar^2}{2m_h}(\nabla_{h_1}^2+\nabla_{h_2}^2)-\frac{e^2}{\epsilon|\mathbf{r}_{e_1}-\mathbf{r}_{h_1}|}$$
$$-\frac{e^2}{\epsilon|\mathbf{r}_{e_1}-\mathbf{r}_{h_2}|}-\frac{e^2}{\epsilon|\mathbf{r}_{e_2}-\mathbf{r}_{h_1}|}-\frac{e^2}{\epsilon|\mathbf{r}_{e_2}-\mathbf{r}_{h_2}|}$$
$$+\frac{e^2}{\epsilon|\mathbf{r}_{e_1}-\mathbf{r}_{e_2}|}+\frac{e^2}{\epsilon|\mathbf{r}_{h_1}-\mathbf{r}_{h_2}|}. \qquad (7)$$

Nair and Takagahara PRB 55,5153(1997)

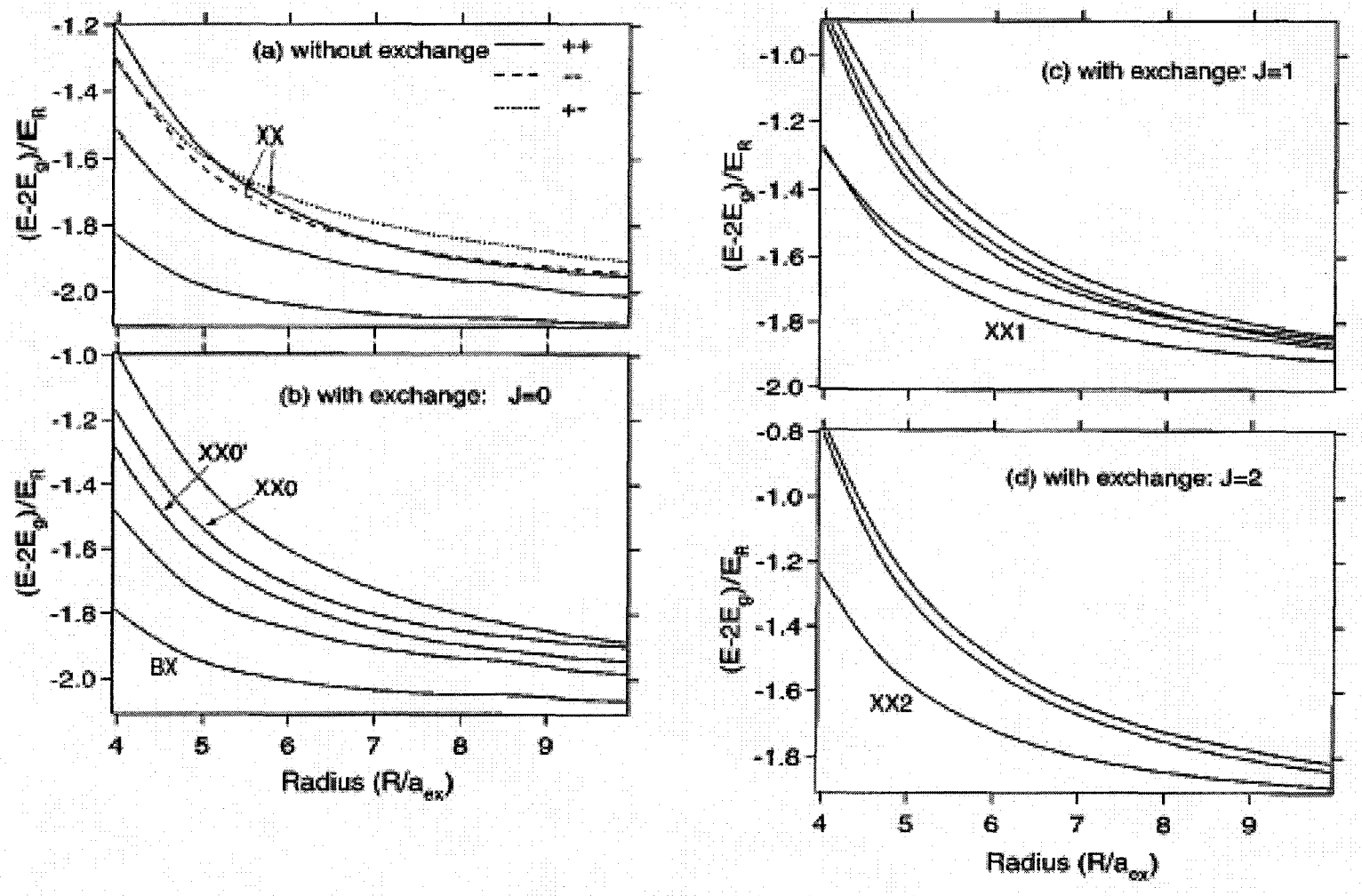

FIG. 2. Calculated energies of the biexciton states (a) without and (b–d) with the electron-hole exchange interaction included. *BX*, *XX*0 (*XX*0′), *XX*1, and *XX*2, respectively, denote the biexciton ground state and the weakly correlated exciton-pair states with $J=0$, 1, and 2. Notations are the same as in Fig. 1.

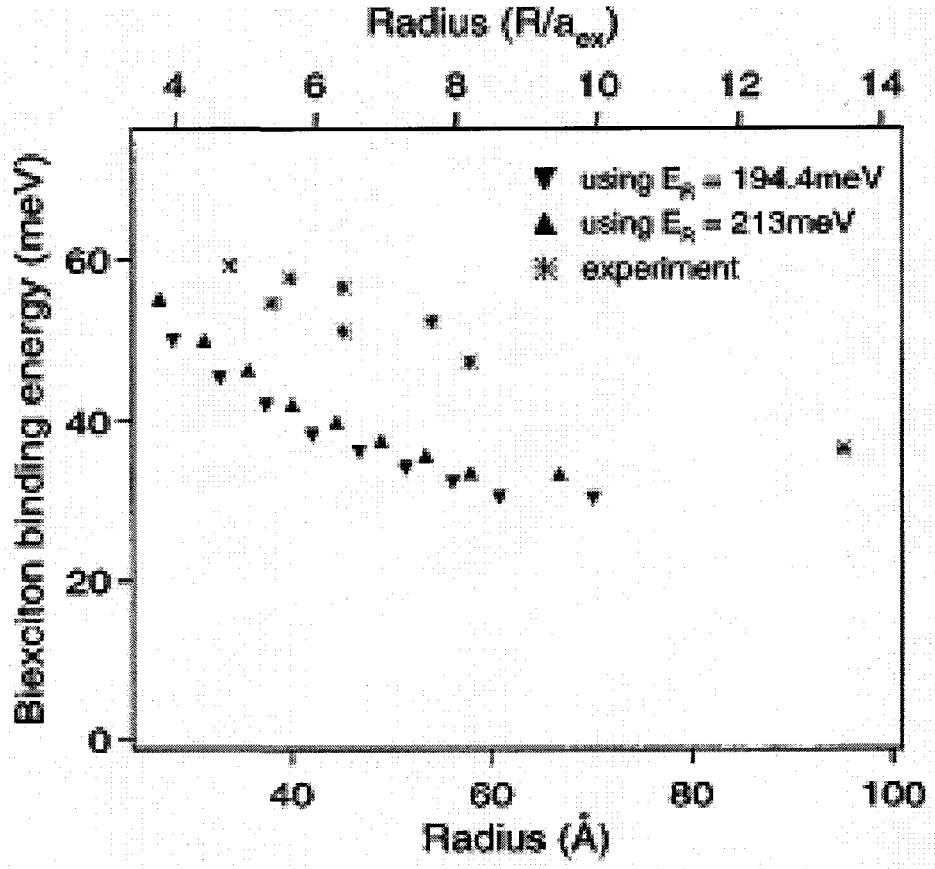

FIG. 3. The calculated size dependence of the biexciton binding energy in CuCl quantum dots. Two sets of results corresponding to the exciton Rydberg $E_R = 194.4$ meV and 213 meV are shown. The experimental results of Ref. 40 are also shown.

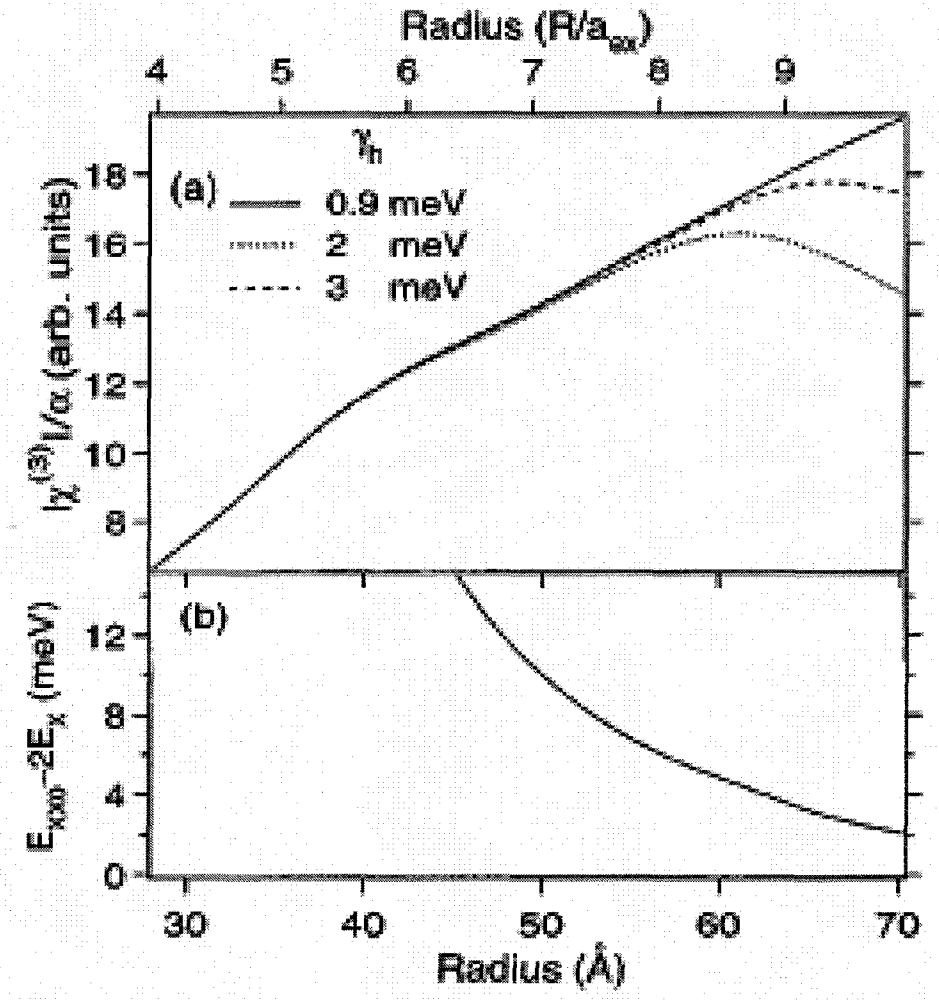

(a) Calculated size dependence of the peak value of (c(3) / a) near the exciton resonance in CuCl QD's. All the curves are scaled to the same value at R=28 Å. The hump seen at R~40 Å arises from the assumed size dependence of γ_h and has no special physical significance. (b) The size dependence of the energy difference between the weakly correlated exciton-pair state (E_{XX0}) and twice the exciton ground state energy (E_X).

Experimental details from K Matsuda et al PRL 91 (2004)

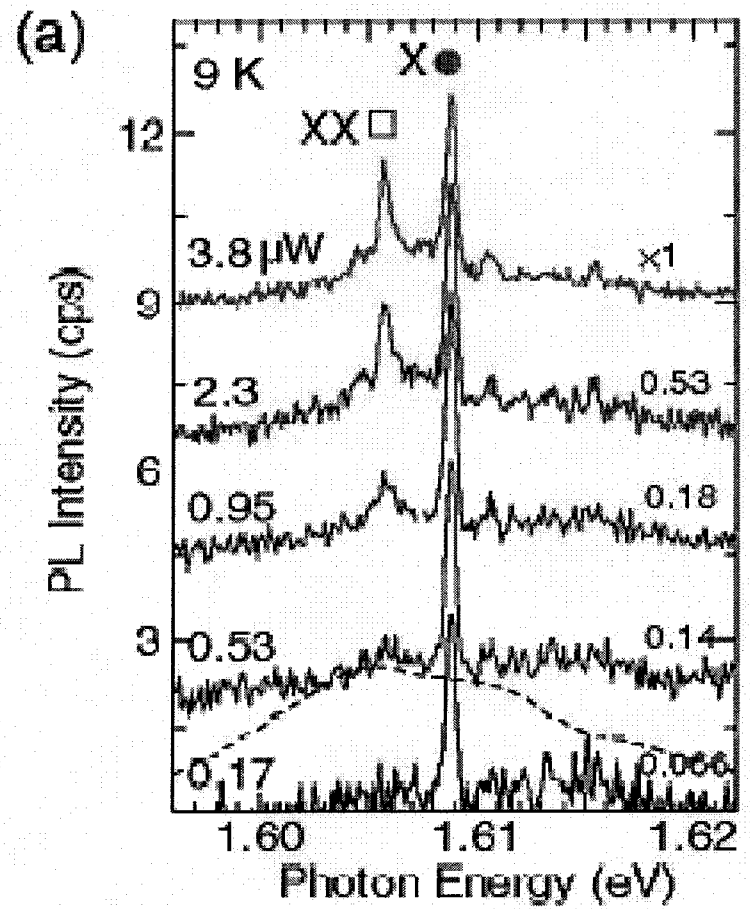

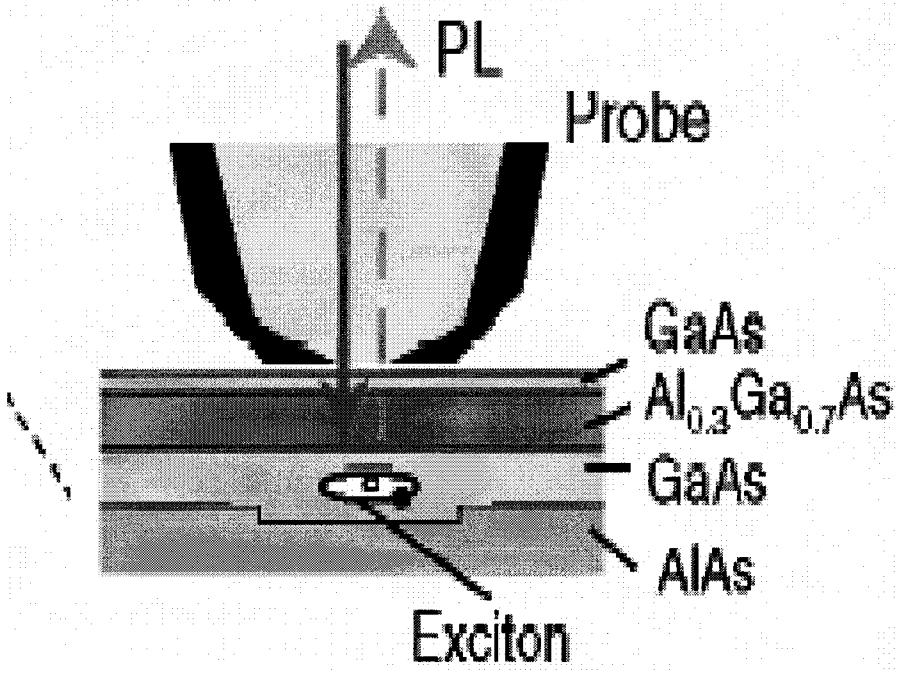

Near-field Optical Mapping of Exciton Wave Functions in a GaAs Quantum dot

K. Matsuda, T. Saiki, S. Nomura, M. Mihara, Y. Aoyagi, S. Nair, and T. Takagahara

Phys. Rev. Lett. **91**, 177401

(issue of 24 October 2003)

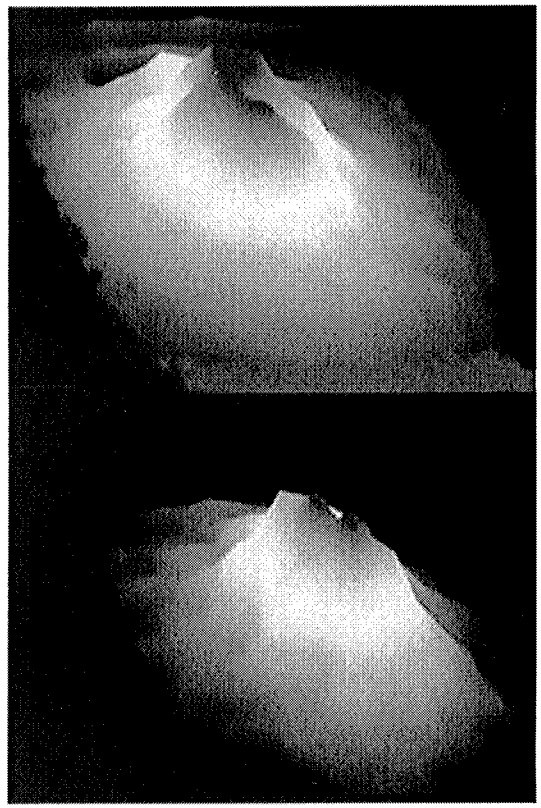

Trapped and tracked. The first images of the motion of an exciton--a particle essential to modern electronics--and a biexciton show that the lighter exciton (top) roams farther.

http://www.physicscentral.com/pictures/pictures-03-10.html

Does quantum confinement enhance nonlinearities?

Inter sub band transitions ~ R

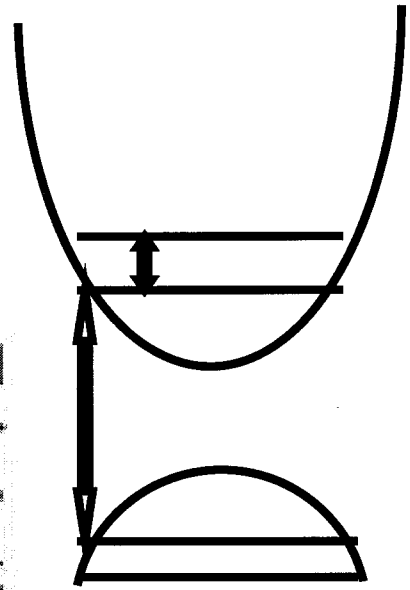

To conclude, we have shown that three-dimensional quantum confinement can alter radically the nonlinear optical properties of semiconductors in the transparency region. The results of this study may have far-reaching consequences for practical devices such as ultrafast optical switches.

$$\chi^{(3)} = \frac{2N\hbar(e/m)^4}{3V\varepsilon_0(\hbar\omega)^4} \sum_{vabc} \rho_{va}\rho_{ab}\rho_{bc}\rho_{cv} \left[\frac{1}{(\Omega_{av}-\omega)(\Omega_{bv}-2\omega)(\Omega_{cv}-\omega)} + \right.$$

5 similar terms

Cotter et al PRL 68,1201(1992)

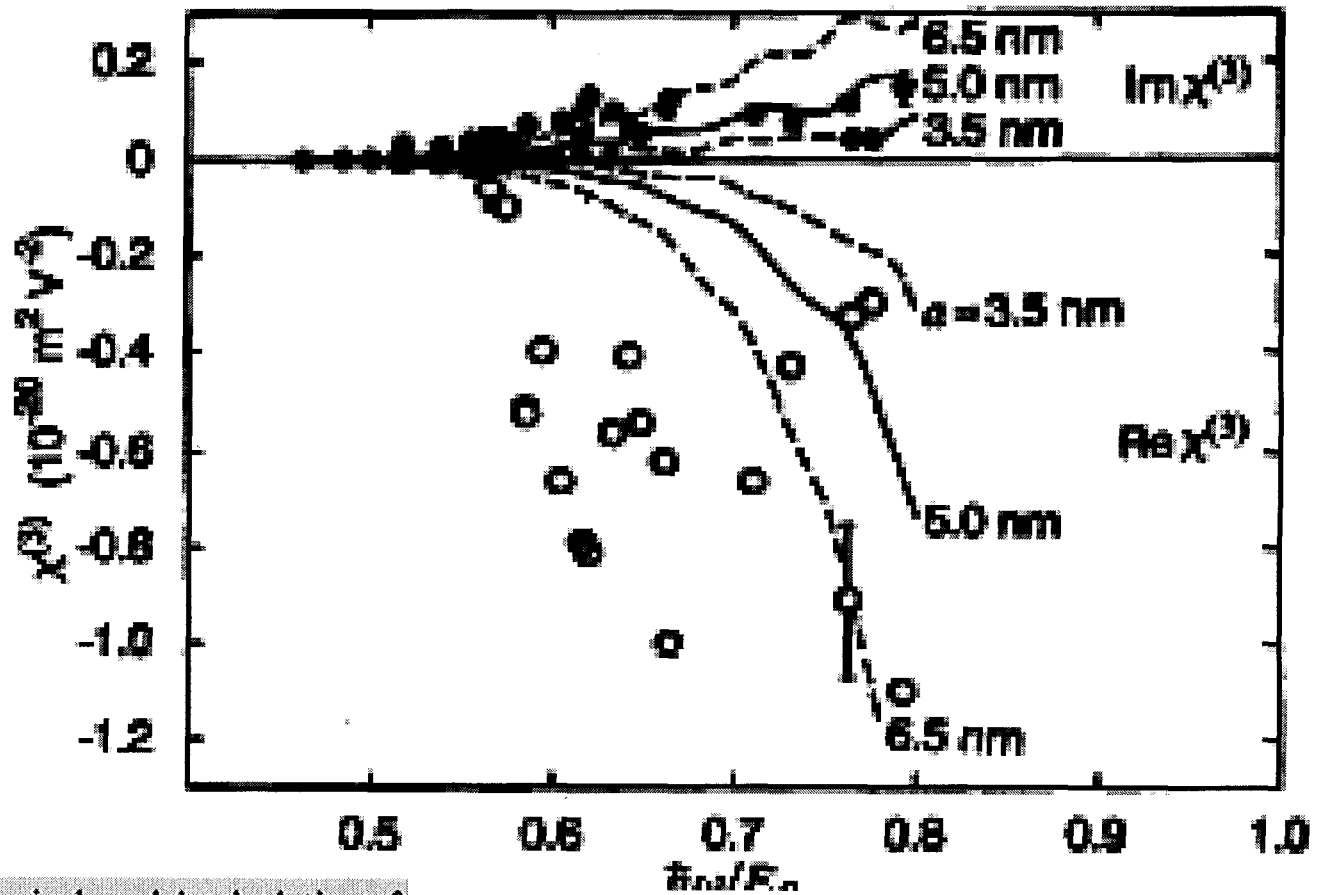

FIG. 1. The solid curves show a typical model calculation of $\chi^{(3)}$ for a sphere of radius $a=5$ nm with $m_c=0.15m$, $m_v=0.8m$, $\hbar\omega=1.17$ eV (1.06 μm), $\Delta E=35$ meV, $|f|^4=0.2$, and $\varepsilon=0.01$. The dashed curves are for the same semiconductor parameters and number density, but different radii a. The curves are plotted vs the normalized photon energy $\hbar\omega/E_0$, taking E_0 as a variable parameter. The distinctive features of these curves are found to be typical of quantum-confined particles (and are robust to changes in parameters), but quite different from those of bulk semiconductors [2]. Values of $\mathrm{Im}\chi^{(3)}$ (solid circles) and $\mathrm{Re}\chi^{(3)}$ (open circles) measured at 1.06-μm wavelength for 24 semiconductor-doped glass samples are shown.

Cotter et al PRL 68,1201(1992)

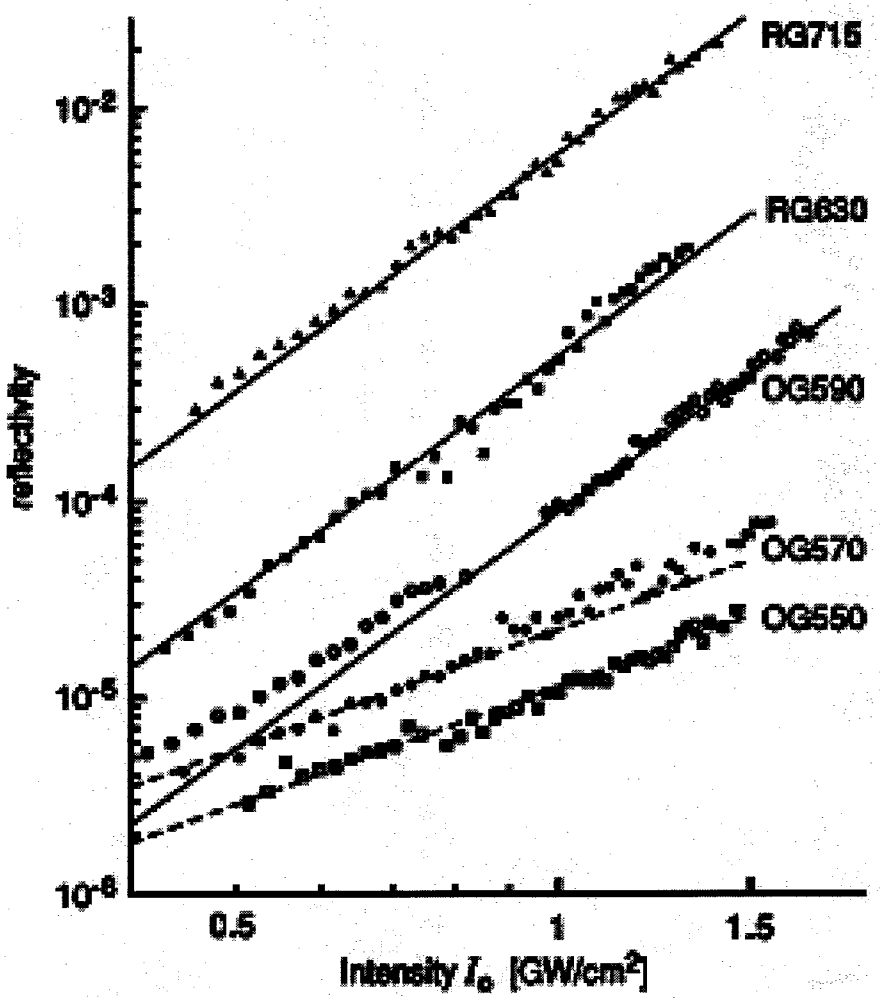

Fig. 2. Reflectivity versus intensity for some SDG's. Data are taken with f, b, and p in temporal coincidence and with parallel polarizations. Sample thickness, 3 mm. Solid lines, $R \propto {I_0}^4$; dotted lines, $R \propto {I_0}^2$. The intensity at the interference maxima of f and b is $\simeq 3.5 \times I_0$.

Banfi et al JOSA B 12,621(1995)

Cotter et al(1992): Semiconductor doped glasses have large third order non-linearity of electronic origin(75ps pulses)

Quantum confinement enhances nonlinearity!

Pavia group: fifth order nonlinearity at relatively low intensities (35 ps pulses)

Bindra

Repeated DFWM and z-scan with 20ps pulses

Nonlinearity apparently fifth order at low intensity third order at higher intensities!

So THE PROBLEM IS REAL!

Resolution:

Nonlinearity is indeed fifth order, but at higher intensities there is saturation of DFWM signal due to nonlinear absorption

Probe beam intensity is much reduced because of Two Photon absorption and linear absorption by the generated ***e,h's***

Similarly , z -scan signal at higher intensities saturates

Bindra et al PRB (1999),Opt Comm (2000)

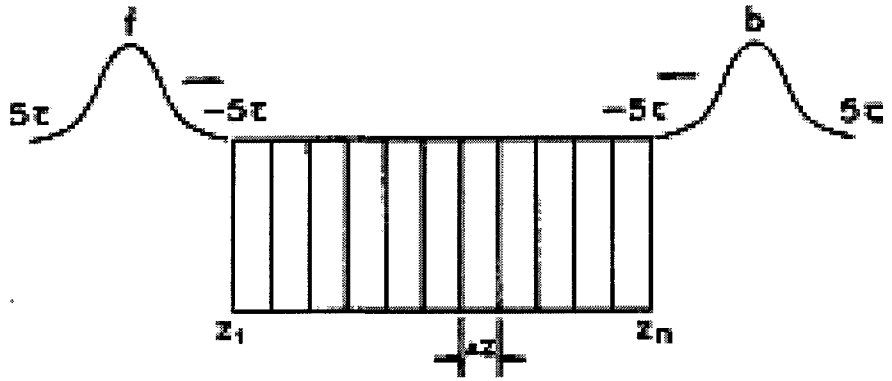

FIG. 7. Sample length is divided into equal segments of thickness Δz. The forward and backward pump beams for $r=0$ at time $t=-5\tau$ are incident on face z_1 and z_n of the sample, respectively.

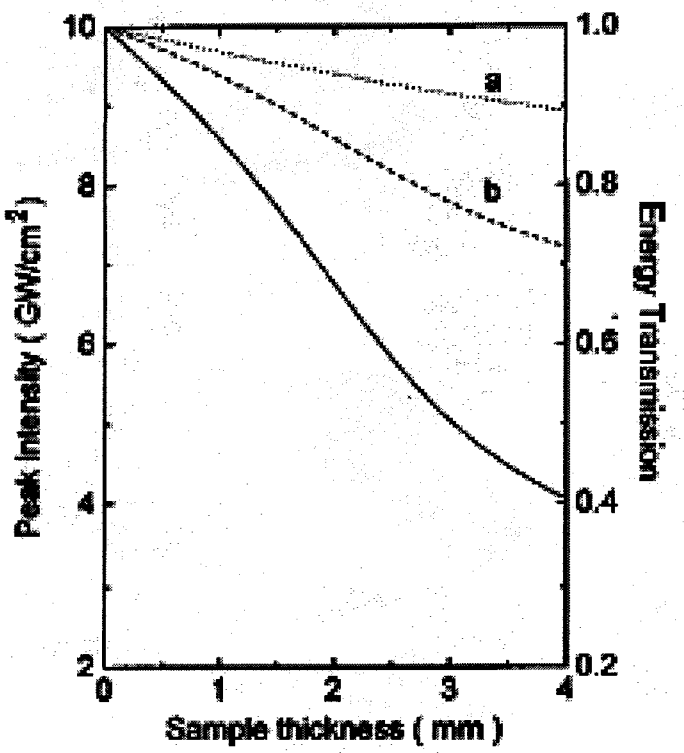

FIG. 3. Energy transmission for forward pump beam (a) when only forward pump beam is present, (b) in the presence of all interacting beams. The solid line shows the reduction of *peak intensity* of forward pump beam in the presence of all beams.

Bindra et al PRB (1999)

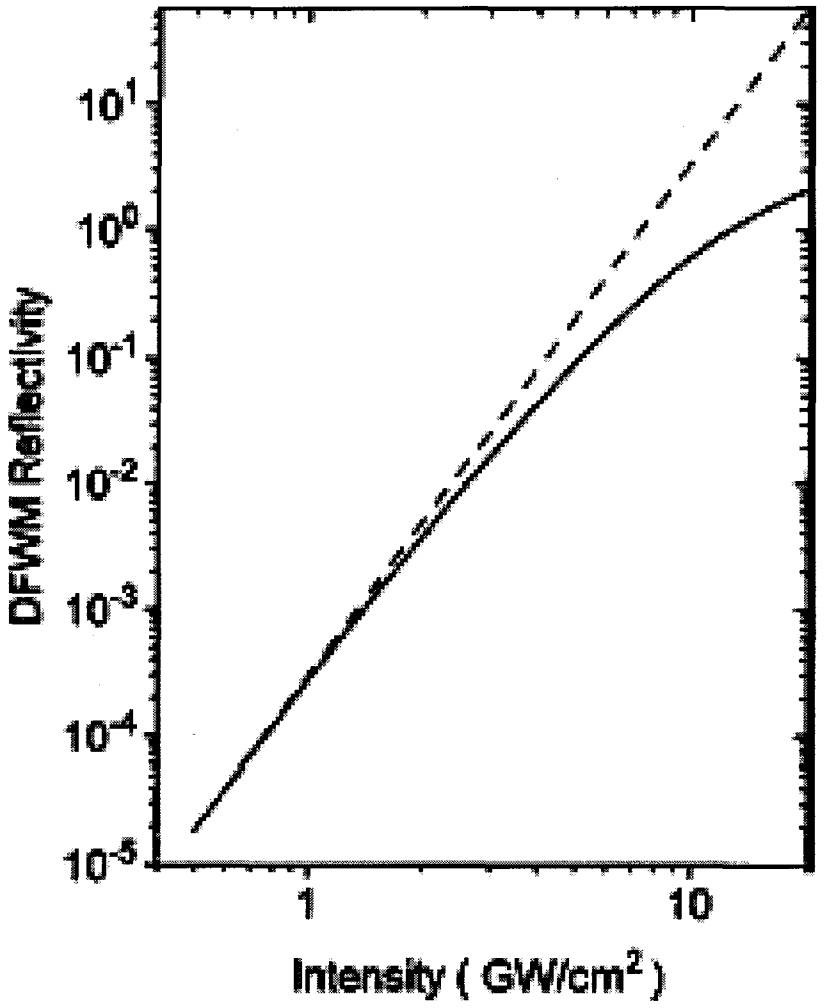

FIG. 4. Phase conjugate reflectivity versus pump intensity estimated with depletion of all interacting beams by nonlinear absorption for filter RG850. Dashes show the I^4 dependence.

Bindra et al PRB (1999)

Intensity dependence

$\Delta n/I$ *and* $T_{p\text{-}v}$

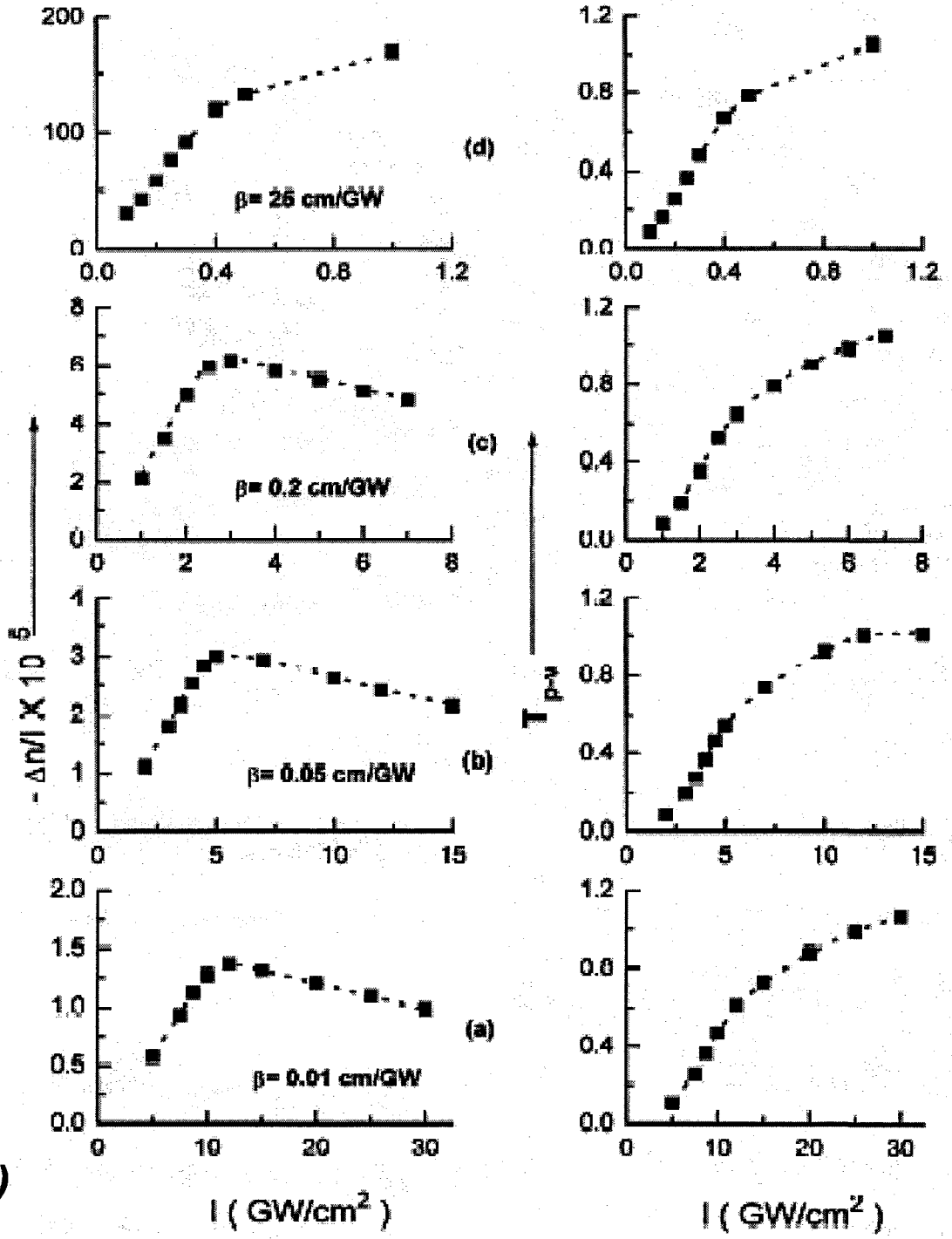

Bindra et al Opt Comm (2000)

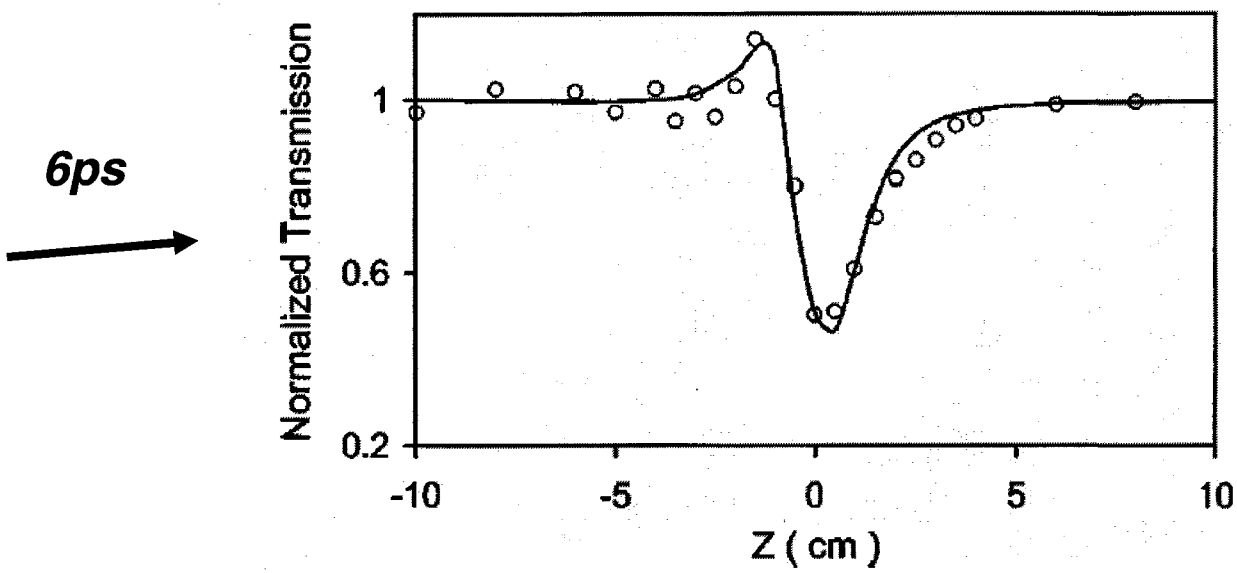

FIG. 1. Closed-aperture z-scan for the sample RG850 with 6 ps pulses.

100 fs

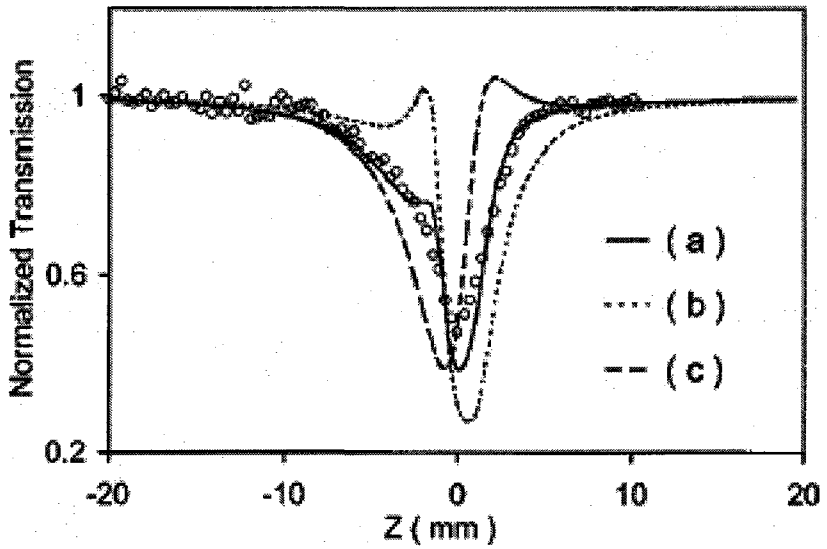

FIG. 3. Closed-aperture z scan for the sample RG850. Circles are the experimental data points. Solid line is the fit obtained with TPA coefficient $=6\times10^{-13}$ mW^{-1}, free carrier cross section$=-1.5\times10^{-22}$ cm^3 and n_2 $=14\times10^{-20}$ m^2W^{-1}. Curve (b) is obtained by neglecting the effect of n_2. Curve (c) is obtained by neglecting the effect of fifth-order nonlinearity.

n_2

TPA generated e-h pairs

Generated carrier absorption

Bindra and Kar APL79,3761(2001)

Intrinsic Optical Bistability

$$E_s = 3E_h/(\varepsilon_s/\varepsilon_h + 2)$$

$$\varepsilon_s/\varepsilon_h = \varepsilon_0 + \gamma|E_s|^2$$

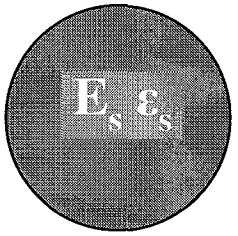

$\mathbf{E_h}$ $\boldsymbol{\varepsilon_h}$

Leung(PRA 1984)

Selfconsistent solutions give optical bistability

Assumed real γ

Rustagi(1997)

$\gamma = |\gamma| e^{i\theta}$

$$\mathrm{Re}((\varepsilon_0 + 2)e^{-i\theta}) < 0$$

$$3|\varepsilon_0 + 2|^2/4 < (\mathrm{Re}(\varepsilon_0 + 2)e^{-i\theta})^2 < |\varepsilon_0 + 2|^2$$

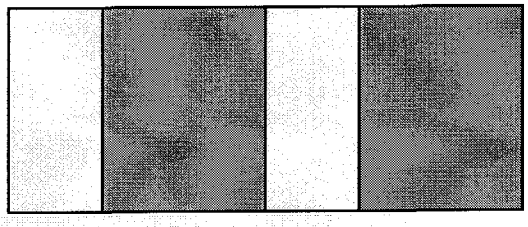

$\alpha\, d + (1 - \alpha) d$

$(\varepsilon_W)_{zz} \quad (\varepsilon_B)_{zz}$

$$E_{1k} = E_1 + \frac{\hbar^2 k^2}{2m^*}$$

$$E_{2k} = E_2 + \frac{\hbar^2 k^2}{2m^*}$$

$$E_{1k} - E_{2k} = E_1 - E_2$$

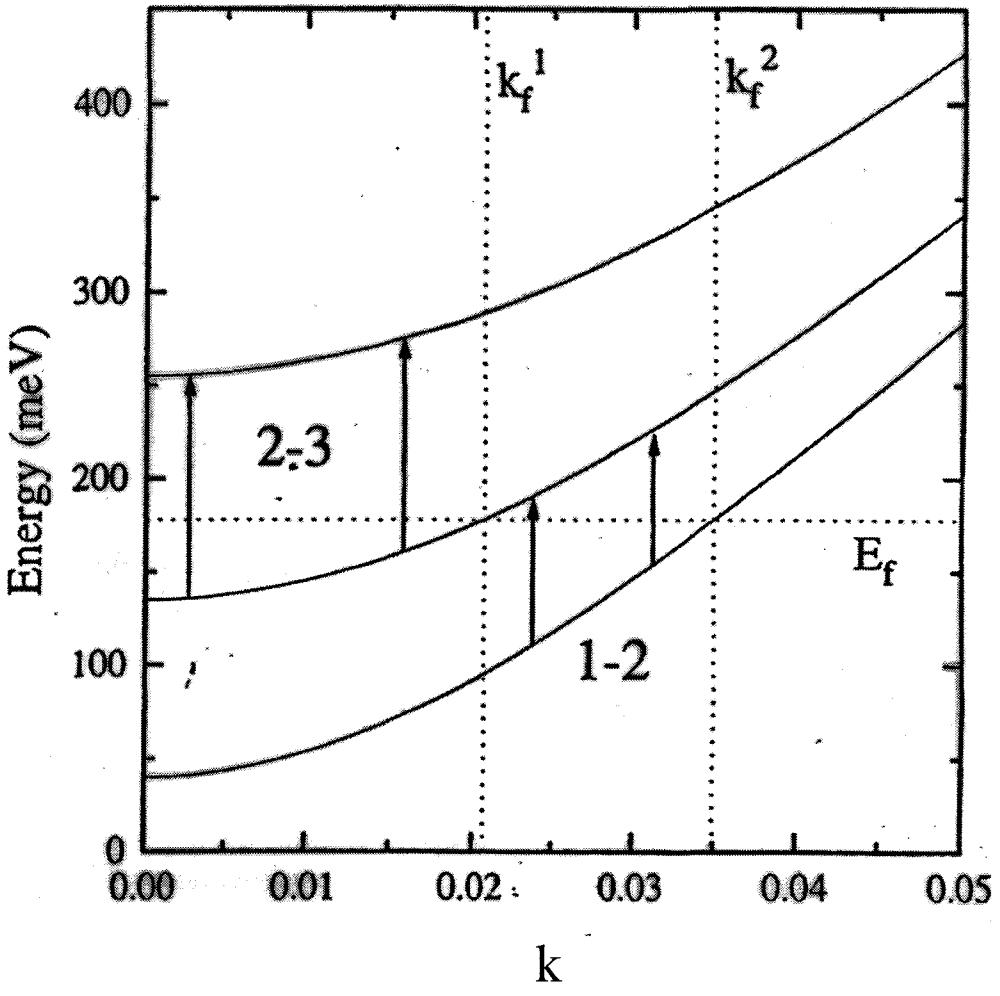

Warburton etal PRL(1998)

effective medium theory : intersub-band resonances

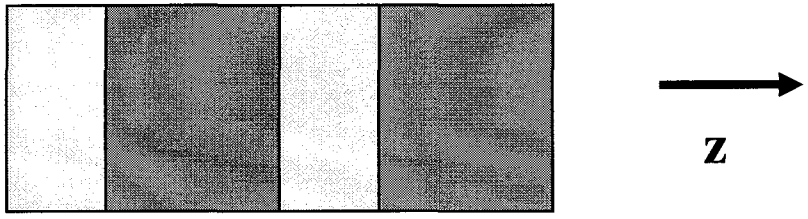

$\alpha\, d + (1 - \alpha) d$

$(\varepsilon_W)_{zz} \quad (\varepsilon_B)_{zz}$

$$1/\langle\varepsilon\rangle = \alpha/\varepsilon_W + (1 - \alpha)/\varepsilon_B$$

$$\varepsilon_W = \varepsilon_{W\,bulk} + \varepsilon_{W\,inter\text{-}sub\text{-}band},$$

$$E_W = \varepsilon_B \langle E\rangle / \{\varepsilon_B \alpha + \varepsilon_W (1 - \alpha)\},$$

$$E_B = \varepsilon_W \langle E\rangle / \{\varepsilon_B \alpha + \varepsilon_W (1 - \alpha)\}$$

$$\langle E\rangle = \alpha E_w + (1 - \alpha) E_B$$

inter-sub-band plasmon : $1/\langle\varepsilon\rangle \rightarrow 0$

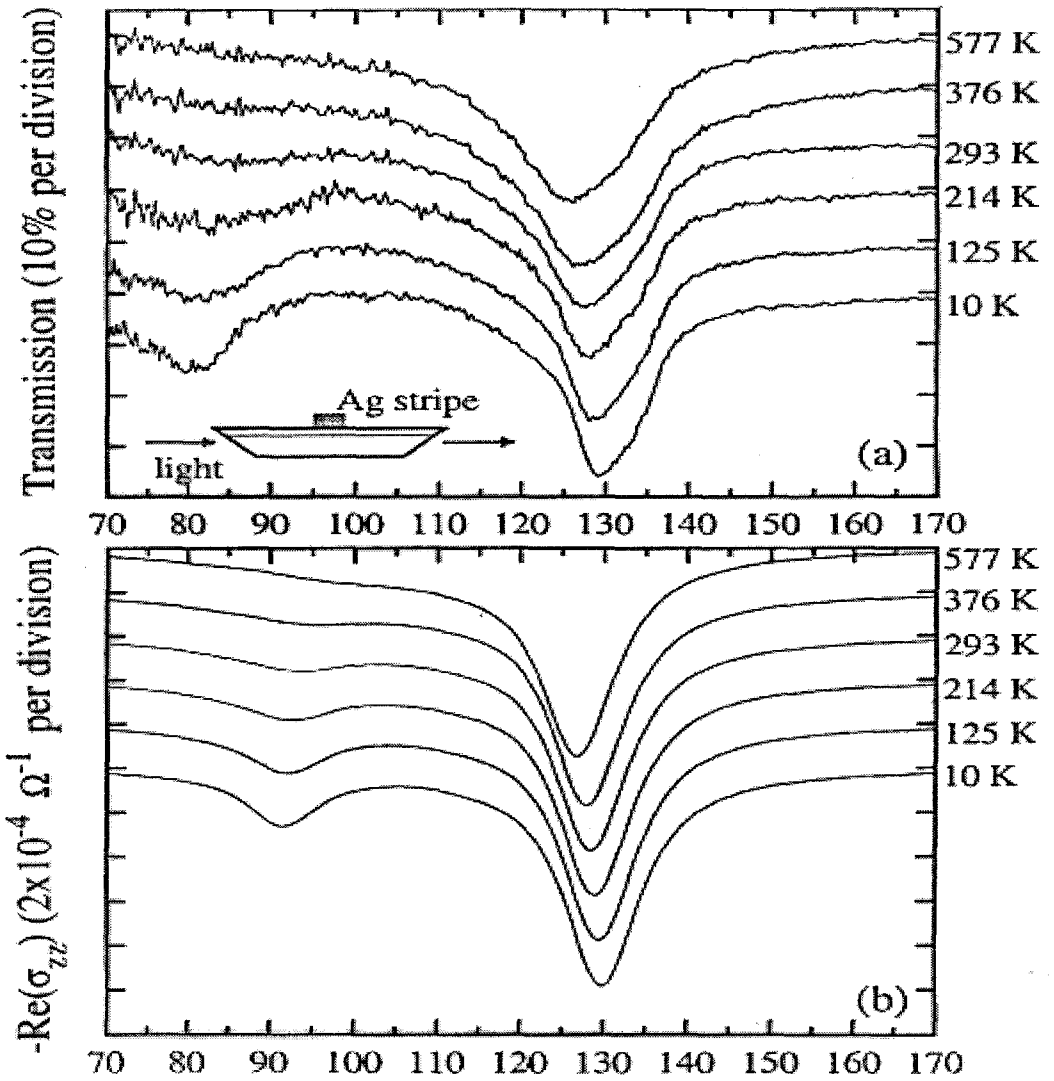

S Mukhopadhyay+KCR(1999)

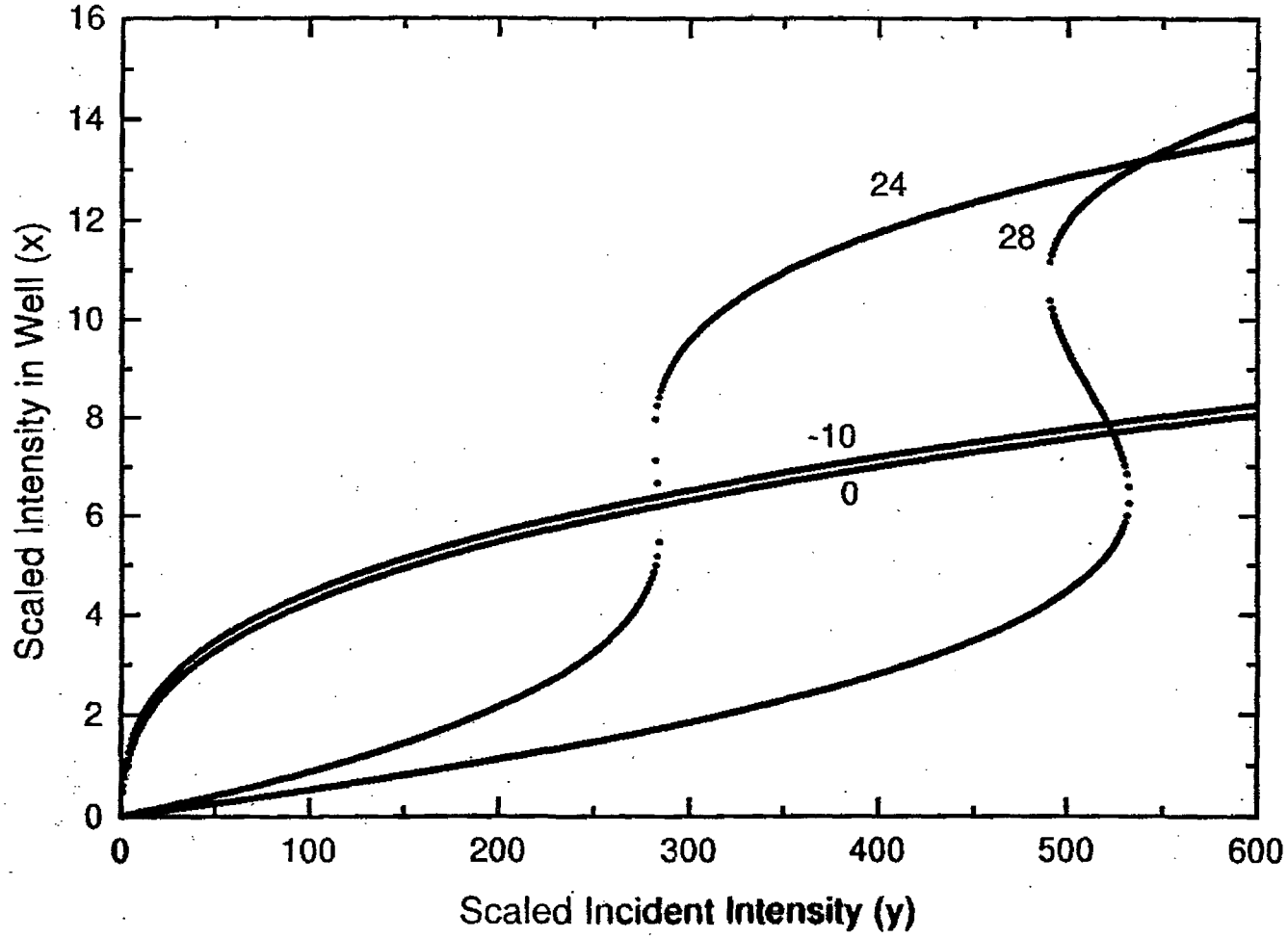

S Mukhopadhyay+KCR(1999)

SUMMARY

EMPIRICAL PSEUDOPOTENTIAL AND TIGHT BINDING CALCULATIONS BECOMING RELIABLE FOR SPHERICAL QUANTUM DOT SPECTRA

SELECTION RULES LESS STRICT FOR SMALL QUANTUM DOTS

NEAR FIELD METHODS EXCITING FOR SINGLE QD SPECTROSCOPY

SHAPE DEPENDENCE OF QUANTUM CONFINEMENT AND DEPOLARIZATION FIELDS IMPORTANT

ACKNOWLEDGEMENTS:

Selvakumar Nair,

Lavanya Ramaniah

K S Bindra

Alka Ingale

J. Jayabalan

References:

H. Kuhn Fortsch Chem Org Nat 16,169(1958), 17,404 (1959)

Semiconductor Quantum Dots - Physics,Spectroscopy and Applications

Y.Masumoto and T.Takagahara (eds) ***Springer (2002)***

One important advantage of the TB theory is that it can treat even non-spherical shapes quite easily, whereas it would be practically impossible to solve the corresponding envelope-function equations.

Nair,Ramaniah,Rustagi PRB 45,5969(1992)